

# Large- $N$ scaling of Tan's contact for the harmonically trapped Tonks–Girardeau gas at finite temperature

Felipe Taha Sant'Ana<sup>1</sup>

<sup>1</sup>*Archimedian, 13560-120, São Carlos, Brazil\**

(Dated: May 27, 2026)

We derive the canonical-ensemble scaling of Tan's contact for  $N$  harmonically trapped Tonks–Girardeau bosons at finite temperature in the large- $N$  limit. The leading scaling coefficient reproduces the local-density-approximation result and is obtained from a contour-integral representation of the canonical partition function followed by a saddle-point reduction to a phase-space integral with a self-consistent scaled chemical potential. The subleading coefficient is the central new object of this work: it admits an explicit representation in terms of universal phase-space integrals of the Fermi factor, has closed-form Sommerfeld and virial limits, and is identified with the canonical-versus-grand-canonical ensemble difference at fixed mean particle number. In the high-temperature Boltzmann regime the ratio of subleading to leading coefficients collapses to a universal value, traceable to the Poissonian particle-number statistics of the dilute grand-canonical gas. We construct Padé approximants for both scaling functions that interpolate uniformly between the low-temperature Sommerfeld and high-temperature virial regimes; for the subleading coefficient we report a form that is uniformly accurate on our working range of temperatures and asymptotically correct beyond. The scaling law is verified against canonical contour-integration data across the full temperature range.

## I. INTRODUCTION

The momentum distribution of strongly interacting quantum gases exhibits a universal  $k^{-4}$  tail at large momentum, with a single proportionality constant—Tan's contact  $\mathcal{C}$ —that controls short-range pair correlations, the interaction energy, the adiabatic sweep theorem and a host of related thermodynamic identities [1–3]. Subsequent derivations of these universal relations using the operator product expansion [4], generalisations to identical bosons [5], and extensions to general dimension and spin [6–9] have established the contact as a unifying observable across the strongly interacting cold-atom landscape, with experimental verifications in three-dimensional Fermi gases [10–12] and in atomic Bose-Einstein condensates [13].

One-dimensional (1D) Bose systems occupy a distinguished place in this landscape because of integrability. The system composed of bosons repulsively interacting through a  $\delta$ -function term is described by the Lieb–Liniger model [14, 15], which remains exactly solvable as long as no external potential is considered, where its finite-temperature thermodynamics is governed by the Yang–Yang equations [16]. In the limit of infinite repulsion the Lieb–Liniger gas reduces to the Tonks–Girardeau (TG) gas, whose hard-core bosons are mapped onto free spinless fermions by the Girardeau construction [17]; yet the TG momentum distribution differs sharply from the Fermi one and exhibits a non-trivial  $k^{-4}$  contact tail. Quasi-one-dimensional geometries are routinely realised by tight transverse confinement and the associated confinement-induced resonance [18], which provides the experimental gateway to the strongly interacting regime; broader context can be found in the review [19].

The TG and Lieb–Liniger regimes have been the subject of an extensive experimental program. Direct observation of TG correlations was reported in optical lattices [20] and in atom-chip and crossed-dipole arrangements [21–23], followed by precision thermometry of 1D Bose gases [24, 25]. More recent experiments have probed strongly interacting 1D dynamics, including dynamical fermionisation [26] and generalised hydrodynamics [27]; very recently, the contact itself has been measured directly in a 1D Lieb–Liniger gas [28], providing a direct quantitative target for theoretical predictions of the contact in terms of the number of particles and the temperature in the trapped geometry.

On the theoretical side, the  $k^{-4}$  tail of the trapped TG gas was identified two decades ago [29], with the corresponding short-distance Lieb–Liniger analysis provided by [30]; the 1D version of Tan's relations has also been systematised [31], and the homogeneous finite-temperature pair correlations were obtained from Yang–Yang thermodynamics by [32]. For the harmonically trapped TG gas at finite temperature, [33] derived a universal scaling through the local density approximation (LDA) within the grand-canonical-ensemble (GCE). Subsequent work has extended this scaling to the trapped Lieb–Liniger gas [34, 35] and to multi-component fermionic mixtures [36, 37], while canonical-ensemble

---

\* felipe@archimedian.ai

corrections relevant to the few-to-many-body crossover have been studied [38, 39]. A unified review of exact-solution methods for strongly interacting trapped 1D quantum gases is given in [40].

In this paper we derive and verify the canonical-ensemble (CE) scaling of Tan’s contact for the harmonically trapped Tonks–Girardeau gas at fixed reduced temperature  $\tau = T/T_F$  and large number of particles. The contact admits a two-term large- $N$  expansion, with a leading contribution of order  $N^{5/2}$  and a subleading correction of order  $N^{3/2}$  governed by two universal  $\tau$ -dependent functions  $A(\tau)$  and  $B(\tau)$ ; the precise scaling law is stated as Eq. (12) at the start of Sec. III. The leading coefficient  $A(\tau)$  coincides with the GCE result of Ref. [33]; we re-derive it from a contour-integral representation of the canonical partition function and provide closed asymptotic expansions in the Sommerfeld ( $\tau \ll 1$ ) and Boltzmann ( $\tau \gg 1$ ) limits. The subleading coefficient  $B(\tau)$  is the focus of the present work: we show that it admits a first-principles saddle-point expression in terms of universal phase-space integrals of the Fermi factor evaluated with a self-consistent scaled chemical potential  $\xi(\tau)$ , that it is precisely the ensemble-difference contribution between the canonical and grand-canonical contacts at fixed mean particle number, and that it admits universal closed asymptotic forms at both low and high temperature. At low temperature  $B(\tau)$  is linear in  $\tau$  with a negative slope, and at high temperature it tends to minus the leading coefficient  $A(\tau)$ , the latter limit following from the Poissonian particle-number statistics of the dilute Boltzmann regime. We construct Padé approximants for  $A(\tau)$  and  $B(\tau)$  that interpolate between the two asymptotic regimes on a wide temperature window, and verify the scaling law against canonical contour-integration data. The result extends the few-body canonical analysis of Ref. [39] and identifies the precise origin of the subleading  $N^{3/2}$  term as a finite- $N$  ensemble-correspondence effect. Read in light of recent direct contact measurements in one-dimensional Lieb–Liniger gases [28], the canonical scaling law provides a quantitative target for trapped-geometry experiments at finite temperature.

The paper is organised as follows. Section III A establishes the canonical contour representation, performs the saddle-point reduction, and derives  $A(\tau)$  together with its asymptotic expansions. Section III B carries out the analogous analysis for the subleading coefficient  $B(\tau)$ , with explicit low- and high- $\tau$  expansions and an explicit evaluation of the boundary-layer “edge” coefficient. Section IV compares the canonical and grand-canonical formulations, identifies  $B(\tau)$  as the ensemble correction, and provides its cumulant interpretation. Numerical procedures, scaling verification, and the Padé approximants are presented in Sec. C 2 and in the dedicated numerical section. We conclude in Sec. V with a summary and outlook.

## II. THE MODEL

We consider  $N$  identical bosons of mass  $m$  on the line, confined by an harmonic potential of frequency  $\omega$  and interacting through a contact potential of coupling strength  $g > 0$ . The Hamiltonian is

$$H = \sum_{i=1}^N \left( -\frac{\hbar^2}{2m} \frac{\partial^2}{\partial x_i^2} + \frac{1}{2} m \omega^2 x_i^2 \right) + g \sum_{i < j} \delta(x_i - x_j). \quad (1)$$

Throughout this paper we work in harmonic-oscillator units, setting  $\hbar = m = \omega = k_B = 1$ , so that lengths are measured in units of the oscillator length  $a_0 = \sqrt{\hbar/m\omega}$ , energies in units of  $\hbar\omega$ , and the single-particle eigenstates of the trap are the familiar Hermite functions

$$\phi_n(x) = \frac{e^{-x^2/2} H_n(x)}{\pi^{1/4} \sqrt{2^n n!}}, \quad \varepsilon_n = n + \frac{1}{2}, \quad n = 0, 1, 2, \dots \quad (2)$$

We restrict our analysis to the Tonks–Girardeau (TG) limit  $g \rightarrow \infty$ , in which the two-body interaction reduces to the impenetrability constraint  $\Psi(x_1, \dots, x_N) = 0$  whenever  $x_i = x_j$  for any  $i \neq j$ . In this limit the Bose–Fermi mapping of Girardeau [17] expresses every bosonic eigenstate as a Slater determinant of single-particle Hermite functions multiplied by an antisymmetrising sign factor,

$$\Psi_\alpha^{(b)}(x_1, \dots, x_N) = \prod_{i < j} \text{sgn}(x_i - x_j) \Psi_\alpha^{(f)}(x_1, \dots, x_N), \quad (3)$$

where  $\Psi_\alpha^{(f)}$  is the noninteracting fermionic Slater determinant labelled by the occupied set  $\alpha = \{n_1, \dots, n_N\}$ . Since  $|\Psi^{(b)}|^2 = |\Psi^{(f)}|^2$ , all local one-body observables of the TG gas (in particular the spatial density and the energy) coincide with those of  $N$  noninteracting spinless fermions in the same trap. Off-diagonal correlations, however, do not: the Bose–Fermi map preserves probability density but not phase, so quantities sensitive to the off-diagonal structure of the one-body density matrix—most notably the momentum distribution—differ remarkably between the two systems [29, 30].

The central object of this work is Tan's contact, defined through the universal large-momentum tail of the single-particle momentum distribution,

$$\mathcal{C} = \lim_{k \rightarrow \infty} k^4 n(k), \quad n(k) = \frac{1}{2\pi} \int dx dx' e^{ik(x-x')} \rho^{(1)}(x, x'), \quad (4)$$

with  $\rho^{(1)}$  the thermal one-body density matrix. The contact admits the formulation as a one-dimensional integral over a positive integrand  $F_N(x)$ <sup>1</sup>,

$$\mathcal{C}_N = \frac{2}{\pi} \int_{-\infty}^{\infty} dx F_N(x), \quad F_N(x) = \langle \rho(x) \kappa(x) - S(x)^2 \rangle_N^{(\text{CE})}, \quad (5)$$

where the local objects  $\rho$ ,  $S$ ,  $\kappa$  are diagonal and near-diagonal values of the fermionic kernel and  $\langle \dots \rangle_N^{(\text{CE})}$  denotes the canonical thermal average at fixed particle number  $N$ . The representation (5) is the starting point for the saddle-point analysis of the following sections.

To compare different particle numbers and temperatures on a common footing, we parametrise the temperature by the dimensionless ratio

$$\tau := \frac{T}{T_F}, \quad T_F = N\hbar\omega, \quad (6)$$

where  $T_F$  is the Fermi temperature of the equivalent noninteracting gas (the energy of the highest occupied harmonic level at  $T = 0$ ). In units with  $\hbar = \omega = k_B = 1$  this reads  $T_F = N$ . At fixed  $\tau$ , the inverse temperature scales as  $\beta := 1/T = 1/(\tau N)$ , so that the thermal de Broglie wavelength  $\lambda_T = \sqrt{2\pi\beta}$  is parametrically smaller than both the oscillator length and the Thomas-Fermi cloud size  $R_{\text{TF}} = \sqrt{2N}$  in the relevant scaling regime. This separation of scales is what makes the large- $N$  expansion at fixed  $\tau$  a genuine semiclassical limit and underlies the  $N^{5/2}$  leading scaling of the contact established in Sec. III A.

The two physically distinct regimes of  $\tau$  correspond to the familiar quantum statistics of a noninteracting Fermi gas:  $\tau \ll 1$  is the deeply degenerate regime in which the Fermi-Dirac distribution is sharp and Sommerfeld-type expansions apply, while  $\tau \gg 1$  is the classical (Boltzmann) regime in which the occupation probabilities are small and the partition function admits a virial expansion. Both limits are accessible analytically and serve as anchors for the finite- $\tau$  analysis that follows. In the intermediate regime  $\tau \sim 1$  we resort to numerical evaluation of the universal scaling functions, supplemented by Padé approximants that interpolate between the two asymptotic forms.

### A. Kernel representation

Let  $\Xi(z)$  be the grand partition function of the trapped ideal Fermi gas,

$$\Xi(z) = \prod_{n \geq 0} (1 + ze^{-\beta\varepsilon_n}). \quad (7)$$

The canonical partition function  $Z_N$  can be extracted through a coefficient analysis of  $z^N$  in  $\Xi(z)$ , admitting the contour representation

$$Z_N = \frac{1}{2\pi i} \oint_{\mathcal{C}} \frac{dz}{z^{N+1}} \Xi(z). \quad (8)$$

The integrand  $F_N(x)$  entering the contact (5) can be written as the corresponding contour average of a grand-canonical kernel functional<sup>2</sup>:

$$F_N(x) = \frac{1}{Z_N} \frac{1}{2\pi i} \oint_{\mathcal{C}} \frac{dz}{z^{N+1}} \Xi(z) [\rho_z(x) \kappa_z(x) - S_z(x)^2], \quad (9)$$

where the kernel  $K_z(x, y)$  and its local derivatives read

$$K_z(x, y) = \sum_{n \geq 0} f_n(z) \phi_n(x) \phi_n(y), \quad f_n(z) = \frac{ze^{-\beta\varepsilon_n}}{1 + ze^{-\beta\varepsilon_n}}, \quad (10)$$

$$\rho_z(x) = K_z(x, x), \quad S_z(x) = \partial_y K_z(x, y)|_{y=x}, \quad \kappa_z(x) = \partial_x \partial_y K_z(x, y)|_{y=x}. \quad (11)$$

<sup>1</sup> See Appendix A for the detailed derivation.

<sup>2</sup> See Appendix B for the detailed derivation.

Figure 1 shows the canonical contact  $\mathcal{C}_N(\tau)$  evaluated from the contour-integral representation for a range of particle numbers; the curves provide the raw data against which the scaling law (12) is verified in later sections.

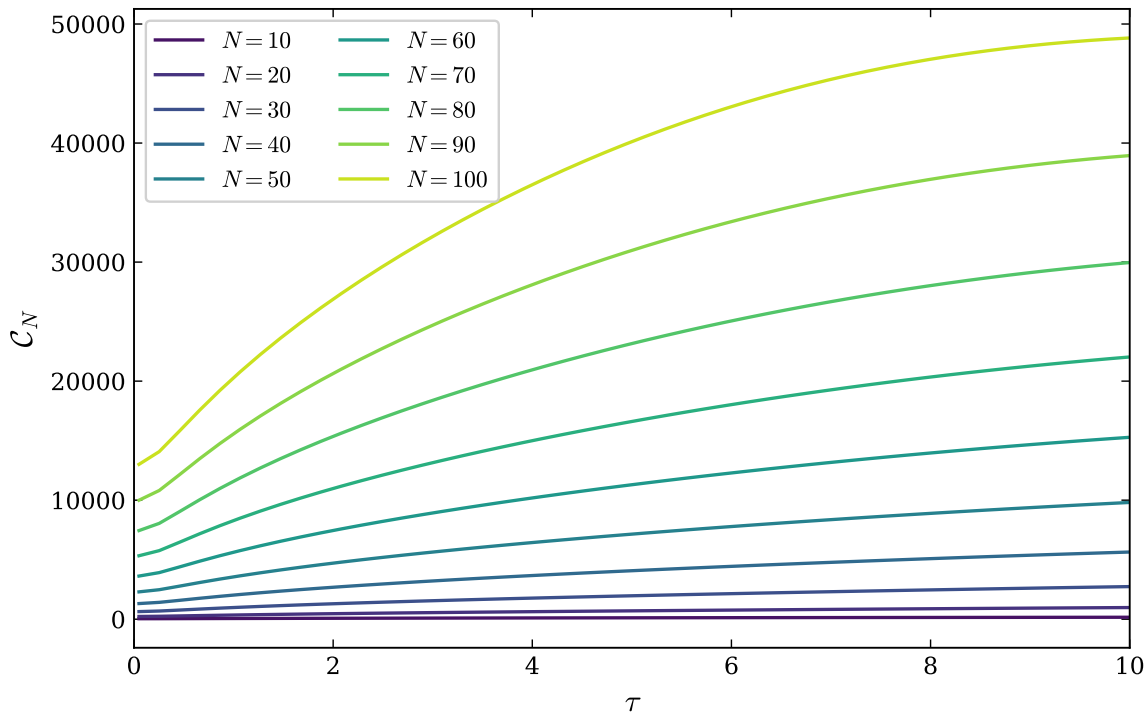


FIG. 1: Canonical-ensemble contact (5) as a function of the reduced temperature  $\tau$ , computed from the contour-integral representation (9). Curves correspond to particle numbers  $N$  from 10 to 100 in steps of 10 (bottom to top). The data underlie the scaling-law verification of Eq. (12).

### III. CANONICAL CONTACT SCALING

In this section we derive the canonical-ensemble large- $N$  scaling law

$$\mathcal{C}_N(\tau) = A(\tau) N^{5/2} + B(\tau) N^{3/2}, \quad (12)$$

through a contour-integral representation of the canonical partition function followed by saddle-point reduction. The leading coefficient  $A(\tau)$  and its asymptotic limits are obtained in Sec. III A; the subleading coefficient  $B(\tau)$ , together with its explicit Sommerfeld and virial expansions, is the subject of Sec. III B.

#### A. Leading term

In order to extract the leading large- $N$  behaviour, we proceed to evaluate both contour integrals in (8) and (9) by the saddle-point method. We begin by writing

$$\frac{\Xi(z)}{z^{N+1}} = \exp[\Phi_N(z)], \quad \Phi_N(z) := \log \Xi(z) - (N+1) \log z. \quad (13)$$

For large  $N$  the  $-\log z$  term is sub-leading and may be dropped at the saddle order: the saddle  $z = z_*$  is determined by

$$\left. \frac{d}{dz} [\log \Xi(z) - N \log z] \right|_{z_*} = 0 \quad \implies \quad N = \sum_{n \geq 0} \frac{z_* e^{-\beta \varepsilon_n}}{1 + z_* e^{-\beta \varepsilon_n}} = \sum_{n \geq 0} f_n(z_*). \quad (14)$$

It is convenient to parametrize  $z_\star = e^{\beta\mu}$ , so that

$$f_n(z_\star) = \frac{1}{e^{\beta(\varepsilon_n - \mu)} + 1}, \quad (15)$$

where  $\mu = \mu(N, T)$  is the chemical potential.

Since both numerator and denominator of (9) are dominated by the same saddle  $z_\star$ , the leading contribution to their ratio is obtained by evaluating the kernel functional at  $z_\star$ :

$$F_N(x) \simeq \rho_{z_\star}(x) \kappa_{z_\star}(x) - S_{z_\star}(x)^2 + \dots, \quad (16)$$

where the displayed equality is asymptotic (the omitted terms are the Gaussian saddle-fluctuation corrections, which we treat systematically in Sec. III B).

We now evaluate  $\rho_{z_\star}(x)$ ,  $\kappa_{z_\star}(x)$  and  $S_{z_\star}(x)$  in the large- $N$ , semiclassical limit at fixed  $\tau$ . In the Wigner, or phase-space, approximation, the kernel becomes local in  $(x, p)$  with Fermi occupation

$$f(p, x) = \frac{1}{e^{\beta\left(\frac{p^2}{2} + V(x) - \mu\right)} + 1}, \quad V(x) = \frac{x^2}{2}. \quad (17)$$

Then the local objects defined in (11) reduce to the moments

$$\rho_{z_\star}(x) \simeq \int_{-\infty}^{\infty} \frac{dp}{2\pi} f(p, x), \quad (18)$$

$$S_{z_\star}(x) \simeq \int_{-\infty}^{\infty} \frac{dp}{2\pi} (ip) f(p, x) = 0, \quad (19)$$

$$\kappa_{z_\star}(x) \simeq \int_{-\infty}^{\infty} \frac{dp}{2\pi} p^2 f(p, x). \quad (20)$$

The vanishing of  $S(x)$  follows from the parity  $p \mapsto -p$  of  $f(p, x)$ .

Using (16) and (19), we obtain

$$F_N(x) \simeq \rho(x) \kappa(x). \quad (21)$$

We now show that (21) implies  $\mathcal{C}_N(\tau) \propto N^{5/2}$ . At fixed  $\tau$  we have  $\beta \sim 1/(\tau N)$ , and the saddle chemical potential  $\mu(N, \tau)$  is fixed by the particle-number constraint (14). Anticipating the scaling  $\mu = \xi(\tau) N$  that will be made explicit shortly, we introduce the standard large- $N$  scaling of coordinates and momenta,

$$x = \sqrt{2N} u, \quad p = \sqrt{2N} q. \quad (22)$$

Then

$$\frac{p^2}{2} + V(x) - \mu = N(q^2 + u^2 - \xi), \quad (23)$$

so that, using  $\beta = 1/(\tau N)$ ,

$$\beta \left( \frac{p^2}{2} + V(x) - \mu \right) = \frac{q^2 + u^2 - \xi}{\tau}. \quad (24)$$

Therefore the occupation (17) becomes  $N$ -independent at leading order,

$$f(p, x) \longrightarrow f_\tau(q, u) := \frac{1}{e^{(q^2 + u^2 - \xi)/\tau} + 1}, \quad \xi = \xi(\tau). \quad (25)$$

The scaled chemical potential  $\xi(\tau)$  is determined self-consistently by the large- $N$  limit of the number constraint (14). Replacing the discrete sum over single-particle levels by an integral against the 1D harmonic oscillator density of states, and using  $\beta = 1/(\tau N)$ ,  $\mu = \xi N$ ,  $\varepsilon_n = NE$  recasts (14) as the transcendental equation

$$\tau \log \left( 1 + e^{\xi/\tau} \right) = 1, \quad \xi = \xi(\tau). \quad (26)$$

Equation (26) admits the asymptotic behaviour  $\xi(\tau \ll 1) = 1 - \tau e^{-1/\tau} + \mathcal{O}(e^{-2/\tau})$  at low temperature and  $\xi(\tau \gg 1) \sim -\tau \log \tau$  at high temperature. The zero-temperature limit  $\xi(0) = 1$  follows directly from (26): as  $\tau \rightarrow 0^+$ ,  $\log(1 + e^{\xi/\tau}) \rightarrow \max(\xi/\tau, 0)$ . Thus the chemical potential coincides with  $N$  at  $T = 0$ ; the corrections at small  $\tau$  are exponentially suppressed and therefore invisible in the Sommerfeld series, while at  $\tau \gtrsim 1$  they grow polynomially and must be retained. For all numerical results below we use the self-consistent  $\xi(\tau)$  from (26): the simpler choice  $\xi = 1$  correctly reproduces the low- $\tau$  Sommerfeld expansion but introduces uncontrolled  $\mathcal{O}(\tau \log \tau)$  errors at  $\tau \gtrsim 1$  that propagate to the universal functions  $A(\tau)$  and  $B(\tau)$ .

Let us begin by defining the dimensionless moments

$$I_0(u; \tau) := \int_{-\infty}^{\infty} dq f_{\tau}(q, u), \quad I_2(u; \tau) := \int_{-\infty}^{\infty} dq q^2 f_{\tau}(q, u). \quad (27)$$

Using  $dp = \sqrt{2N} dq$  and (18)–(20) gives

$$\rho(x) \simeq \int \frac{dp}{2\pi} f(p, x) = \frac{\sqrt{2N}}{2\pi} I_0(u; \tau), \quad (28)$$

$$\kappa(x) \simeq \int \frac{dp}{2\pi} p^2 f(p, x) = \frac{(2N)^{3/2}}{2\pi} I_2(u; \tau). \quad (29)$$

Inserting (28) and (29) into (21) yields

$$F_N(x) \simeq \rho(x)\kappa(x) = \frac{(2N)^2}{4\pi^2} I_0(u; \tau) I_2(u; \tau) = \frac{N^2}{\pi^2} I_0(u; \tau) I_2(u; \tau). \quad (30)$$

Finally, using the definition of the contact (4), we obtain the large- $N$  limit leading scaling term

$$\begin{aligned} \mathcal{C}_N(\tau) &\simeq \frac{2}{\pi} \int_{-\infty}^{\infty} dx \frac{N^2}{\pi^2} I_0(u; \tau) I_2(u; \tau) \\ &= \frac{2}{\pi} \sqrt{2N} \frac{N^2}{\pi^2} \int_{-\infty}^{\infty} du I_0(u; \tau) I_2(u; \tau) \\ &= A(\tau) N^{5/2}, \end{aligned} \quad (31)$$

where we defined the universal scaling function  $A(\tau)$  as

$$A(\tau) := \frac{2\sqrt{2}}{\pi^3} \int_{-\infty}^{\infty} du I_0(u; \tau) I_2(u; \tau), \quad (32)$$

with  $I_0, I_2$  given by (27) and  $f_{\tau}$  by (25).

### 1. Low-temperature

In the zero-temperature limit,  $f_{\tau}(q, u) \rightarrow \Theta(1 - u^2 - q^2)$ . Then for  $|u| < 1$ ,

$$I_0(u; 0) = 2\sqrt{1 - u^2}, \quad I_2(u; 0) = \frac{2}{3}(1 - u^2)^{3/2}, \quad I_0 I_2 = \frac{4}{3}(1 - u^2)^2, \quad (33)$$

and  $I_0 = I_2 = 0$  for  $|u| > 1$ . Therefore

$$\int_{-\infty}^{\infty} du I_0(u; 0) I_2(u; 0) = \frac{4}{3} \int_{-1}^1 du (1 - u^2)^2 = \frac{64}{45}, \quad (34)$$

which gives

$$A(0) = \frac{128\sqrt{2}}{45\pi^3}, \quad (35)$$

reproducing the known  $T = 0$  coefficient.

We now proceed to work out the subleading correction to  $A(\tau)$  in the low- $\tau$  regime, i.e. the Sommerfeld expansion around  $\tau = 0$ . Note that for each fixed finite  $\tau \geq 0$ , the integrals defining  $A(\tau)$  are finite. In the low- $\tau$  expansion we ignore exponentially small corrections to  $\xi(\tau)$  — recall  $\xi(\tau \ll 1) = 1 - \tau e^{-1/\tau} + \mathcal{O}(e^{-2/\tau})$  from (26) — and replace  $\xi$  by its zero-temperature value  $\xi(0) = 1$  throughout the algebraic Sommerfeld series. The neglected pieces enter the contact only at  $\mathcal{O}(e^{-1/\tau})$  and are therefore invisible in the polynomial expansion. The Fermi factor in (25) depends on  $q$  only through  $q^2 - a$ , with  $a := 1 - u^2$ . For  $|u| < 1$  we have  $a = 1 - u^2 > 0$  and we can use the standard Sommerfeld expansion<sup>3</sup>, yielding, for  $|u| < 1$  (i.e.  $a > 0$ ),

$$\begin{aligned} I_0(u; \tau) I_2(u; \tau) &= \left( 2\sqrt{a} - \frac{\pi^2 \tau^2}{12} a^{-3/2} \right) \left( \frac{2}{3} a^{3/2} + \frac{\pi^2 \tau^2}{12} a^{-1/2} \right) \\ &= \frac{4}{3} (1 - u^2)^2 + \frac{\pi^2}{9} \tau^2. \end{aligned} \quad (37)$$

Remarkably, the  $\tau^2$  term is independent of  $u$  in the bulk region  $|u| < 1$ . For  $|u| > 1$  the quantity  $a = 1 - u^2 < 0$  and both  $I_0$  and  $I_2$  are exponentially small in  $1/\tau$ ; moreover, the turning-point region  $|u| \approx 1$  has width  $\Delta u \sim \tau$  and contributes only  $\mathcal{O}(\tau^3)$  to the  $u$  integral, hence it does not affect the  $\tau^2$  coefficient. Finally, we find

$$\begin{aligned} \int_{-\infty}^{\infty} du I_0(u; \tau) I_2(u; \tau) &= \frac{4}{3} \int_{-1}^1 du (1 - u^2)^2 + \frac{\pi^2}{9} \tau^2 \int_{-1}^1 du \\ &= \frac{64}{45} + \frac{2\pi^2}{9} \tau^2. \end{aligned} \quad (38)$$

Therefore,

$$A(\tau) = \frac{2\sqrt{2}}{\pi^3} \left( \frac{64}{45} + \frac{2\pi^2}{9} \tau^2 \right) = \underbrace{\frac{128\sqrt{2}}{45\pi^3}}_{A(0)} + \underbrace{\frac{4\sqrt{2}}{9\pi}}_{a_2} \tau^2, \quad (\tau \ll 1). \quad (39)$$

It is sometimes convenient to write the correction in relative form:

$$A(\tau) = A(0) \left[ 1 + \frac{a_2}{A(0)} \tau^2 + \dots \right] = A(0) \left[ 1 + \frac{5\pi^2}{32} \tau^2 \right], \quad A(0) = \frac{128\sqrt{2}}{45\pi^3}. \quad (40)$$

Equivalently, the low- $\tau$  expansion of the leading large- $N$  contact reads

$$\mathcal{C}_N(\tau) = \frac{128\sqrt{2}}{45\pi^3} N^{5/2} \left( 1 + \frac{5\pi^2}{32} \tau^2 \right). \quad (41)$$

## 2. High temperature

For  $\tau \gg 1$  the saddle fugacity is small and the gas is in the Boltzmann regime. Writing the Fermi factor (25) as

$$f_\tau(q, u) = \frac{1}{z^{-1} e^{(q^2+u^2)/\tau} + 1}, \quad z := e^{\xi/\tau}, \quad (42)$$

the LDA number constraint (26) reads  $\tau \log(1+z) = 1$ , hence  $z = e^{1/\tau} - 1 = 1/\tau + \mathcal{O}(1/\tau^2) \ll 1$  at high  $\tau$ . Using the virial (small- $z$ ) series

$$f_\tau(q, u) = z e^{-(q^2+u^2)/\tau} - z^2 e^{-2(q^2+u^2)/\tau} + \mathcal{O}(z^3), \quad (43)$$

the moments (27) reduce to elementary Gaussian integrals. Writing

$$I_0(u; \tau) = z G_1(u; \tau) - z^2 G_2(u; \tau) + \mathcal{O}(z^3), \quad I_2(u; \tau) = z H_1(u; \tau) - z^2 H_2(u; \tau) + \mathcal{O}(z^3), \quad (44)$$

<sup>3</sup> For a smooth function  $g(\varepsilon)$ ,

$$\int_0^\infty d\varepsilon g(\varepsilon) \frac{1}{e^{(\varepsilon-a)/\tau} + 1} = \int_0^a d\varepsilon g(\varepsilon) + \frac{\pi^2 \tau^2}{6} g'(a) + \mathcal{O}(\tau^4), \quad (a > 0). \quad (36)$$

the Gaussian moments read

$$G_1 = \sqrt{\pi\tau} e^{-u^2/\tau}, \quad G_2 = \sqrt{\pi\tau/2} e^{-2u^2/\tau}, \quad H_1 = \frac{\sqrt{\pi}}{2} \tau^{3/2} e^{-u^2/\tau}, \quad H_2 = \frac{\sqrt{\pi}}{2} \tau^{3/2} 2^{-3/2} e^{-2u^2/\tau}. \quad (45)$$

Hence

$$\begin{aligned} g_0(u; \tau) &:= I_0(u; \tau) I_2(u; \tau) = z^2 G_1 H_1 - z^3 (G_1 H_2 + G_2 H_1) + \mathcal{O}(z^4) \\ &= \frac{\pi}{2} \tau^2 z^2 e^{-2u^2/\tau} - \frac{\pi}{2} \tau^2 z^3 \frac{3}{2\sqrt{2}} e^{-3u^2/\tau} + \mathcal{O}(z^4). \end{aligned} \quad (46)$$

Integrating over  $u$  we have

$$\int du g_0(u; \tau) = \frac{\pi^{3/2}}{2\sqrt{2}} \tau^{5/2} z^2 \left( 1 - \frac{\sqrt{3}}{2} z \right) + \mathcal{O}(z^4). \quad (47)$$

Plugging (47) into (32) yields

$$A(\tau) = \frac{\tau^{5/2}}{\pi^{3/2}} z^2 \left( 1 - \frac{\sqrt{3}}{2} z \right). \quad (48)$$

At  $\tau \gg 1$ , the number constraint in scaled variables gives

$$\frac{1}{\tau} = z - \frac{1}{2} z^2 + \mathcal{O}(z^3) \quad \implies \quad z = \frac{1}{\tau} + \frac{1}{2\tau^2} + \mathcal{O}\left(\frac{1}{\tau^3}\right). \quad (49)$$

Inserting (49) into (48):

$$\tau^{5/2} z^2 = \sqrt{\tau} \left( 1 + \frac{1}{\tau} + \mathcal{O}(\tau^{-2}) \right), \quad 1 - \frac{\sqrt{3}}{2} z = 1 - \frac{\sqrt{3}}{2\tau} + \mathcal{O}(\tau^{-2}), \quad (50)$$

so that, multiplying the two expansions to relative order  $1/\tau$ ,

$$A(\tau) = \frac{\sqrt{\tau}}{\pi^{3/2}} \left( 1 + \frac{2 - \sqrt{3}}{2\tau} + \mathcal{O}(\tau^{-2}) \right), \quad (\tau \gg 1). \quad (51)$$

## B. Subleading term

To extract the subleading  $N^{3/2}$  correction we go beyond the leading saddle evaluation (16) of the canonical contour representation (9) and include the Gaussian fluctuations around the saddle. Introducing the saddle variable

$$t := \log z \quad (z = e^t, \quad dz = e^t dt), \quad (52)$$

and writing

$$\psi(t) := \log \Xi(e^t), \quad \Phi(t) := \psi(t) - Nt, \quad (53)$$

both contour integrals become Laplace integrals,<sup>4</sup> with saddle  $\Phi'(t_*) = 0$  recovering the number constraint (14) and Fermi factors (15) at  $z_* = e^{t_*} = e^{\beta\mu}$ . Expanding  $\Phi$  and  $\tilde{G}(t; x) := G(e^t; x)$  around  $t_*$ , the standard Laplace ratio expansion yields

$$F_N(x) = \tilde{G}_*(x) - \frac{1}{2} \frac{\tilde{G}_2(x)}{\Phi_2} + \frac{1}{2} \frac{\Phi_3}{\Phi_2^2} \tilde{G}_1(x) + R_N(x), \quad (54)$$

---

<sup>4</sup> The symbol  $\Phi$  also appears later as the universal edge functions  $\Phi_0(y), \Phi_2(y)$  of (80); the saddle action  $\Phi(t)$  used here, a function of  $t = \log z$ , is unrelated. Subscripts  $\Phi_k = \Phi^{(k)}(t_*)$  in this subsection denote derivatives of the saddle action, while the subscripts on  $\Phi_0, \Phi_2$  in Sec. III B denote moment orders.

with  $\Phi_k = \Phi^{(k)}(t_\star)$  and  $\tilde{G}_k = \partial_t^k \tilde{G}|_{t_\star}$ . The remainder  $R_N(x)$  is suppressed by an additional factor of  $1/\Phi_2 \sim 1/N$  relative to the displayed corrections, i.e.  $R_N = \mathcal{O}(\tilde{G}_\star/N^2)$  in absolute terms or  $\mathcal{O}(N^{-2})$  relative to the leading  $\tilde{G}_\star$ . Since  $\psi(t)$  is the cumulant generating function of the grand-canonical particle number,  $\Phi_2$  and  $\Phi_3$  are themselves particle-number cumulants:

$$\Phi_2 = \kappa_2 = \sum_{n \geq 0} f_n(1 - f_n), \quad \Phi_3 = \kappa_3 = \sum_{n \geq 0} f_n(1 - f_n)(1 - 2f_n), \quad (55)$$

both of which scale as  $\mathcal{O}(N)$  at fixed  $\tau$ , making the two displayed correction terms in (54) of relative order  $1/N$  compared to  $\tilde{G}_\star$  (absolute order  $\tilde{G}_\star/N$ ).

In the fixed- $\tau$  scaling limit, parity again kills  $S(x)$  and the leading saddle functional reduces, via (28) and (29), to

$$\tilde{G}_\star(x) \simeq \rho(x)\kappa(x) \simeq \frac{N^2}{\pi^2} g_0(u; \tau), \quad (56)$$

with  $I_0, I_2$  given by (27)<sup>5</sup>. The dependence of the Fermi factor (25) on  $t = \beta\mu$  enters only through  $f_\tau$ , with

$$\partial_t f_\tau = f_\tau(1 - f_\tau), \quad \partial_t^2 f_\tau = f_\tau(1 - f_\tau)(1 - 2f_\tau), \quad (57)$$

so differentiation under the  $q$ -integral introduces the local integrals

$$J_0(u; \tau) := \int_{-\infty}^{\infty} dq f_\tau(1 - f_\tau), \quad J_2(u; \tau) := \int_{-\infty}^{\infty} dq q^2 f_\tau(1 - f_\tau), \quad (58)$$

$$K_0(u; \tau) := \int_{-\infty}^{\infty} dq f_\tau(1 - f_\tau)(1 - 2f_\tau), \quad K_2(u; \tau) := \int_{-\infty}^{\infty} dq q^2 f_\tau(1 - f_\tau)(1 - 2f_\tau). \quad (59)$$

Using  $\partial_t I_\alpha = J_\alpha$ ,  $\partial_t^2 I_\alpha = K_\alpha$  and  $g_0 = I_0 I_2$ ,

$$\partial_t g_0 = J_0 I_2 + I_0 J_2, \quad (60)$$

$$\partial_t^2 g_0 = K_0 I_2 + 2J_0 J_2 + I_0 K_2. \quad (61)$$

Importantly, a phase-space replacement of the discrete sums in (55) converts the cumulants into global  $u$ -integrals,

$$\kappa_2 \simeq \frac{N}{\pi} V_2(\tau), \quad V_2(\tau) := \int_{-\infty}^{\infty} du J_0(u; \tau), \quad (62)$$

$$\kappa_3 \simeq \frac{N}{\pi} V_3(\tau), \quad V_3(\tau) := \int_{-\infty}^{\infty} du K_0(u; \tau). \quad (63)$$

Inserting (56)–(63) into (54) gives us

$$F_N(x) = \frac{N^2}{\pi^2} g_0(u; \tau) - \frac{N}{\pi} \mathcal{H}(u; \tau), \quad (64)$$

with

$$\mathcal{H}(u; \tau) := \frac{1}{2} \left[ \frac{\partial_t^2 g_0(u; \tau)}{V_2(\tau)} - \frac{V_3(\tau)}{V_2(\tau)^2} \partial_t g_0(u; \tau) \right]. \quad (65)$$

Therefore, inserting (64) into (5) and integrating (with  $dx = \sqrt{2N} du$ ) then yields the canonical scaling law (12) with  $A(\tau)$  as in (32) and the new universal subleading function

$$B(\tau) = -\frac{2\sqrt{2}}{\pi^2} \int_{-\infty}^{\infty} du \mathcal{H}(u; \tau). \quad (66)$$

---

<sup>5</sup> With the leading scaling  $\tilde{G}_\star \sim N^2$  established in (56), the displayed corrections are  $\mathcal{O}(N)$  in absolute terms, and the remainder  $R_N = \mathcal{O}(1)$ .

Substituting (60)–(65) into (66), we obtain the explicit form

$$B(\tau) = \frac{\sqrt{2}}{\pi^2} \int_{-\infty}^{\infty} du \left[ \frac{V_3(\tau)}{V_2(\tau)^2} (J_0 I_2 + I_0 J_2) - \frac{K_0 I_2 + 2J_0 J_2 + I_0 K_2}{V_2(\tau)} \right], \quad (67)$$

which expresses the subleading coefficient entirely in terms of universal phase-space integrals of the Fermi factor, valid for all  $\tau \geq 0$ .

For the numerical verification of the scaling law (12) carried out throughout the rest of the paper, it is convenient to introduce the dimensionless ratio

$$\mathcal{R}_N(\tau) := \frac{\mathcal{C}_N(\tau)}{A(\tau) N^{5/2} + B(\tau) N^{3/2}}, \quad (68)$$

which satisfies  $\mathcal{R}_N(\tau) \rightarrow 1$  as  $N \rightarrow \infty$  at fixed  $\tau$ , with relative deviation  $\mathcal{O}(N^{-1})$  controlled by the next-to-subleading  $N^{1/2}$  correction. We now evaluate (67) in the asymptotic limits  $\tau \ll 1$  and  $\tau \gg 1$ .

### 1. Low-temperature

In the bulk region  $|u| < 1$ , with  $a := 1 - u^2 > 0$ , the moments (27) admit the standard Sommerfeld expansion

$$I_0(u; \tau) = 2\sqrt{a} - \frac{\pi^2 \tau^2}{12} a^{-3/2} + \mathcal{O}(\tau^4), \quad I_2(u; \tau) = \frac{2}{3} a^{3/2} + \frac{\pi^2 \tau^2}{12} a^{-1/2} + \mathcal{O}(\tau^4). \quad (69)$$

Using the identity  $f_\tau(1 - f_\tau) = \tau [-\partial_\varepsilon f_\tau]$  with  $\varepsilon = q^2$  in (58), together with the Sommerfeld formula

$$\int_0^\infty d\varepsilon g(\varepsilon) f_\tau(1 - f_\tau) = \tau \left[ g(a) + \frac{\pi^2 \tau^2}{6} g''(a) + \mathcal{O}(\tau^4) \right], \quad (a > 0), \quad (70)$$

and the analogous identity  $f_\tau(1 - f_\tau)(1 - 2f_\tau) = \tau^2 \partial_\varepsilon^2 f_\tau$  for (59), we obtain

$$J_0 = \tau a^{-1/2} + \mathcal{O}(\tau^3), \quad J_2 = \tau a^{1/2} + \mathcal{O}(\tau^3), \quad (71)$$

$$K_0 = -\frac{1}{2} \tau^2 a^{-3/2} + \mathcal{O}(\tau^4), \quad K_2 = \frac{1}{2} \tau^2 a^{-1/2} + \mathcal{O}(\tau^4), \quad (72)$$

valid for  $|u| < 1$  away from the turning points. Substituting (69)–(72) into (60)–(61) the leading-order coefficients combine into

$$\partial_t g_0(u; \tau) = \frac{8}{3} \tau a + \mathcal{O}(\tau^3), \quad \partial_t^2 g_0(u; \tau) = \frac{8}{3} \tau^2 + \mathcal{O}(\tau^4), \quad (73)$$

where, remarkably, the  $\tau^2$  term in  $\partial_t^2 g_0$  is  $u$ -independent in the bulk and the would-be  $\tau^4$  correction cancels exactly in the combination  $K_0 I_2 + 2J_0 J_2 + I_0 K_2$ .

The global functions (62)–(63) are most cleanly evaluated as two-dimensional phase-space integrals. Setting  $u = r \cos \theta$ ,  $q = r \sin \theta$ , the Fermi factor depends only on  $r^2$ ; substituting  $s = r^2$  and then  $y = (s - 1)/\tau$  converts  $V_2, V_3$  into one-dimensional integrals over the Fermi function  $f(y) = (e^y + 1)^{-1}$ . Using  $f'(y) = -f(y)(1 - f(y))$ ,

$$V_2(\tau) = \pi \tau f(-1/\tau) = \pi \tau \left[ 1 + \mathcal{O}(e^{-1/\tau}) \right], \quad (74)$$

and from  $f(1 - f)(1 - 2f) = -(d/dy)[f(1 - f)]$ , we have

$$V_3(\tau) = \pi \tau f(-1/\tau) [1 - f(-1/\tau)] = \pi \tau e^{-1/\tau} \left[ 1 + \mathcal{O}(e^{-1/\tau}) \right]. \quad (75)$$

Thus  $V_3(\tau)$  is nonperturbatively small: it vanishes to all algebraic orders in the Sommerfeld expansion. Consequently  $V_3/V_2^2 \sim \mathcal{O}(e^{-1/\tau}/\tau)$ , and the entire  $V_3$ -term in (65) contributes only  $\mathcal{O}(e^{-1/\tau})$  to  $B(\tau)$ ; its algebraic expansion is therefore controlled solely by  $\partial_t^2 g_0/V_2$ .

Combining (73) and (74) in (65) gives, for  $|u| < 1$ ,

$$\mathcal{H}(u; \tau) = \frac{4}{3\pi} \tau + \mathcal{O}(\tau^3) + \mathcal{O}(e^{-1/\tau}), \quad (76)$$

which is  $u$ -independent in the bulk. Inserting (76) into (66) and integrating over  $u \in [-1, 1]$  yields the leading low- $\tau$  behaviour

$$B(\tau) = -\frac{16\sqrt{2}}{3\pi^3} \tau + (\text{edge}) + \mathcal{O}(\tau^3) + \mathcal{O}(e^{-1/\tau}). \quad (77)$$

The bulk Sommerfeld formulae (72) are not uniform at the turning points  $u = \pm 1$ , where  $a \rightarrow 0$ : the negative powers of  $a$  diverge, signalling a boundary layer of width  $1 - u^2 \sim \tau$  that must be resolved separately. For that, we introduce the edge scaling variable

$$y := \frac{1 - u^2}{\tau}, \quad u = \sqrt{1 - \tau y}, \quad du = -\frac{\tau dy}{2\sqrt{1 - \tau y}} \xrightarrow{\tau \rightarrow 0} -\frac{\tau}{2} dy, \quad (78)$$

and rescale momenta by  $q = \sqrt{\tau} p$ , so that  $q^2 + u^2 - \xi(\tau) = \tau(p^2 - y) + \mathcal{O}(\tau e^{-1/\tau})$  when  $\xi(\tau) = 1 + \mathcal{O}(e^{-1/\tau})$ . The Fermi factor reduces to the universal,  $\tau$ -independent form

$$f_\tau(\sqrt{\tau} p, u) \xrightarrow{\tau \rightarrow 0} f_y(p) := \frac{1}{e^{p^2 - y} + 1}. \quad (79)$$

Defining the edge functions

$$\Phi_0(y) := \int_{-\infty}^{\infty} dp f_y(p), \quad \Phi_2(y) := \int_{-\infty}^{\infty} dp p^2 f_y(p), \quad (80)$$

and using the identity  $\partial_t = z \partial_z = \tau \partial_\xi$  at fixed  $u$ , which in edge variables becomes  $\partial_t \rightarrow \partial_y$  (a shift in  $\xi$  by  $\delta\xi$  shifts  $y$  by  $\delta\xi/\tau$ , and  $\partial_t = \tau \partial_\xi$ , so the two factors of  $\tau$  cancel). Combined with  $dq = \sqrt{\tau} dp$ , this gives the systematic edge scaling

$$\begin{aligned} I_0 &= \sqrt{\tau} \Phi_0(y), & I_2 &= \tau^{3/2} \Phi_2(y), \\ J_0 &= \sqrt{\tau} \Phi'_0(y), & J_2 &= \tau^{3/2} \Phi'_2(y), \\ K_0 &= \sqrt{\tau} \Phi''_0(y), & K_2 &= \tau^{3/2} \Phi''_2(y). \end{aligned} \quad (81)$$

Substituting (81) into the combination appearing in  $\partial_t^2 g_0$  gives us

$$K_0 I_2 + 2J_0 J_2 + I_0 K_2 = \tau^2 [\Phi''_0 \Phi_2 + 2\Phi'_0 \Phi'_2 + \Phi_0 \Phi''_2] = \tau^2 \mathcal{P}''(y), \quad \mathcal{P}(y) := \Phi_0(y) \Phi_2(y), \quad (82)$$

i.e. the combination collapses to the second derivative of a single universal function. Similarly the cumulant from (74) is uniform in  $u$  at this order, so the integration in  $\int du \partial_t^2 g_0 / V_2$  collects the boundary correction.

We compute this  $u$ -integral by matched asymptotic subtraction. Splitting the  $u$ -integration domain symmetrically and substituting (78) near  $u = +1$ ,

$$\begin{aligned} \int_{-1}^1 du \partial_t^2 g_0(u; \tau) &= 2 \int_0^1 du \partial_t^2 g_0(u; \tau) \\ &= 2 \int_0^1 du \frac{8\tau^2}{3} + 2 \int_0^1 du \left[ \partial_t^2 g_0(u; \tau) - \frac{8\tau^2}{3} \right] \\ &= \frac{16\tau^2}{3} + \tau^3 \int_0^\infty dy \left[ \mathcal{P}''(y) - \frac{8}{3} \right] + \mathcal{O}(\tau^4). \end{aligned} \quad (83)$$

The first term is the uniform bulk Sommerfeld contribution  $(8/3)\tau^2$  integrated over  $|u| < 1$ ; the second is the boundary correction. As  $y \rightarrow \infty$ ,  $\Phi_0(y) = 2\sqrt{y} + \mathcal{O}(y^{-3/2})$  and  $\Phi_2(y) = (2/3)y^{3/2} + \mathcal{O}(y^{-1/2})$  (the standard Sommerfeld expansion of the universal edge function at large argument), so  $\mathcal{P}(y) = (4/3)y^2 + \text{const} + \mathcal{O}(y^{-1})$  and  $\mathcal{P}''(y) = 8/3 + \mathcal{O}(y^{-3})$ : the subtraction makes the integrand decay fast enough at infinity for the integral to converge. Writing  $\mathcal{P}''(y) - 8/3 = (d/dy)[\mathcal{P}'(y) - (8/3)y]$  and integrating by parts,

$$\int_0^\infty dy \left[ \mathcal{P}''(y) - \frac{8}{3} \right] = \left[ \mathcal{P}'(y) - \frac{8}{3}y \right]_0^\infty = -\mathcal{P}'(0), \quad (84)$$

where the upper limit vanishes because the Sommerfeld expansion of  $\mathcal{P}(y)$  at large  $y$  has no  $\mathcal{O}(y)$  term in  $\mathcal{P}'$ . Finally, we have for (66):

$$B(\tau) = -\frac{16\sqrt{2}}{3\pi^3} \tau + b_{\text{edge}} \tau^2 + \mathcal{O}(\tau^3) + \mathcal{O}(e^{-1/\tau}), \quad b_{\text{edge}} = \frac{\sqrt{2}}{\pi^3} \mathcal{P}'(0). \quad (85)$$

To express  $\mathcal{P}'(0)$  in closed form, recall the complete Fermi–Dirac integral

$$F_\nu(\eta) := \frac{1}{\Gamma(\nu+1)} \int_0^\infty \frac{t^\nu}{e^{t-\eta} + 1} dt, \quad F'_\nu(\eta) = F_{\nu-1}(\eta), \quad (86)$$

which is convergent as a Riemann integral for  $\nu > -1$  and extended to  $\nu < -1$  by analytic continuation in  $\nu$  (the explicit formulae below for  $F_{-1/2}$  and  $F_{-3/2}$  at the origin are understood in that sense; see e.g. Cloutman [41] or Dingle [42]). Substituting  $t = p^2$  in (80),

$$\Phi_0(y) = \sqrt{\pi} F_{-1/2}(y), \quad \Phi_2(y) = \frac{\sqrt{\pi}}{2} F_{1/2}(y), \quad (87)$$

so that, using  $F'_\nu(\eta) = F_{\nu-1}(\eta)$ ,

$$\mathcal{P}'(0) = \Phi'_0(0)\Phi_2(0) + \Phi_0(0)\Phi'_2(0) = \frac{\pi}{2} [F_{-3/2}(0)F_{1/2}(0) + F_{-1/2}(0)^2]. \quad (88)$$

Applying the closed-form value

$$F_\nu(0) = \frac{1 - 2^{-\nu}}{\Gamma(\nu+1)} \zeta(\nu+1) \quad (89)$$

to  $\nu = -3/2, -1/2, 1/2$  yields

$$b_{\text{edge}} = -\frac{\sqrt{2}}{4\pi^3} \left[ (1 - 2\sqrt{2})(2 - \sqrt{2}) \zeta\left(-\frac{1}{2}\right) \zeta\left(\frac{3}{2}\right) - 2(1 - \sqrt{2})^2 \zeta\left(\frac{1}{2}\right)^2 \right]. \quad (90)$$

Finally, combining (85) and (90), we have the explicit small- $\tau$  expansion of the subleading coefficient

$$B(\tau) = -\frac{16\sqrt{2}}{3\pi^3} \tau - \frac{\sqrt{2}}{4\pi^3} \left[ (1 - 2\sqrt{2})(2 - \sqrt{2}) \zeta\left(-\frac{1}{2}\right) \zeta\left(\frac{3}{2}\right) - 2(1 - \sqrt{2})^2 \zeta\left(\frac{1}{2}\right)^2 \right] \tau^2. \quad (91)$$

## 2. High temperature

For  $\tau \gg 1$  the saddle fugacity is small,  $z = e^{\beta\mu} \ll 1$ , and the Fermi factor (25) is uniformly dilute in the relevant phase-space region. To leading order in the fugacity,

$$f_\tau(1 - f_\tau) \simeq f_\tau, \quad f_\tau(1 - f_\tau)(1 - 2f_\tau) \simeq f_\tau, \quad (92)$$

so  $J_\alpha \simeq I_\alpha$  and  $K_\alpha \simeq I_\alpha$ . Combined with (60)–(61) this gives

$$\partial_t g_0 \simeq 2g_0, \quad \partial_t^2 g_0 \simeq 4g_0, \quad (93)$$

and at the global level  $V_3(\tau) \simeq V_2(\tau)$ . Substituting into (65),

$$\mathcal{H}(u; \tau) \simeq \frac{1}{2} \left[ \frac{4g_0}{V_2} - \frac{2g_0}{V_2} \right] = \frac{g_0(u; \tau)}{V_2(\tau)}, \quad (94)$$

so that, by (66) and the definition (32) of  $A(\tau)$ ,

$$B(\tau) \simeq -\pi \frac{A(\tau)}{V_2(\tau)}. \quad (95)$$

In the dilute regime the grand-canonical particle-number distribution becomes Poissonian, so  $\kappa_2 \simeq \langle N \rangle$ , which through (62) fixes

$$V_2(\tau) \xrightarrow{\tau \rightarrow \infty} \pi. \quad (96)$$

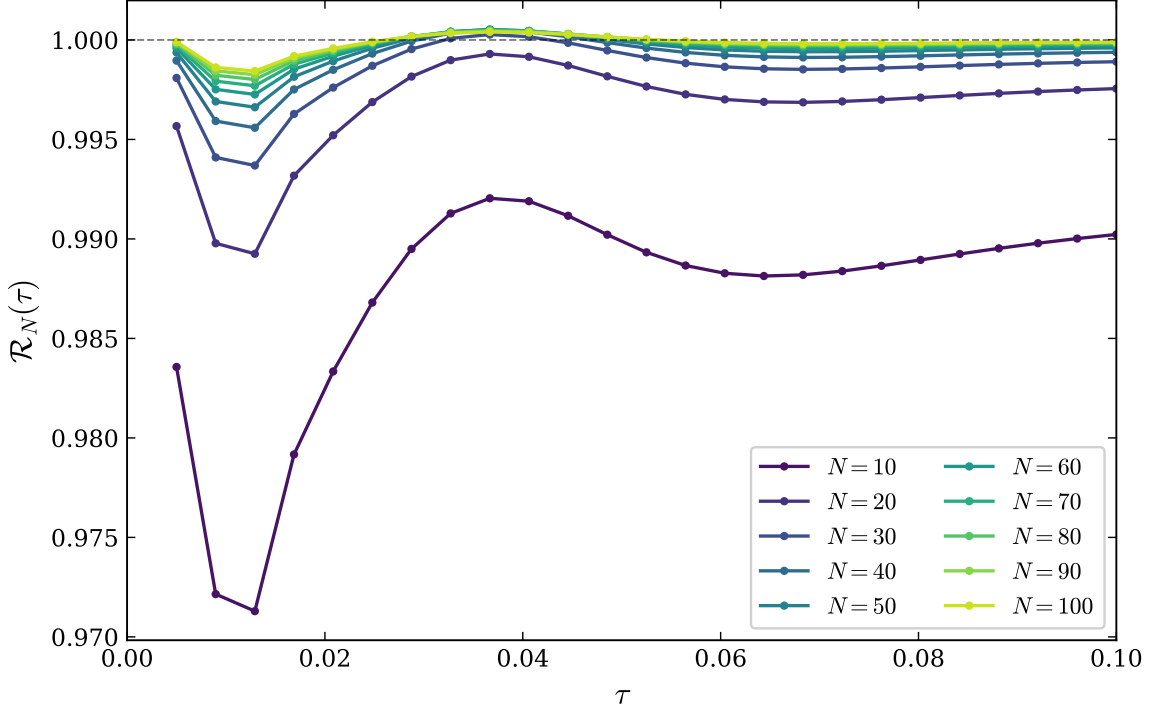


FIG. 2: Low- $\tau$  verification of the canonical scaling law (12). The ratio  $\mathcal{R}_N$  defined in (68), with  $A(\tau)$  and  $B(\tau)$  obtained from the universal integral representations (32) and (67) using the self-consistent scaled chemical potential  $\xi(\tau)$  from (26), is plotted on  $\tau \in [0.005, 0.1]$  for  $N = 10, \dots, 100$ . Convergence to unity (dashed line) confirms the leading and subleading scaling at low temperature, including the Sommerfeld coefficient  $a_2 = 4\sqrt{2}/(9\pi)$  in (39) and the linear-in- $\tau$  leading behaviour  $B(\tau) \simeq -(16\sqrt{2}/3\pi^3)\tau$  in (91).

Combining (95), (96) with the high- $\tau$  leading asymptote of  $A(\tau)$  from (51),

$$B(\tau) \xrightarrow{\tau \rightarrow \infty} -A(\tau) = -\frac{\sqrt{\tau}}{\pi^{3/2}}, \quad (97)$$

so  $\mathcal{C}_N(\tau) \sim (\sqrt{\tau}/\pi^{3/2})N^{5/2} - (\sqrt{\tau}/\pi^{3/2})N^{3/2} + \dots$ . Thus, in the Boltzmann regime, the canonical  $N^{3/2}$  correction is equal in magnitude and opposite in sign to the leading  $N^{5/2}$  coefficient—a universal ratio  $B/A \rightarrow -1$  that we revisit in Sec. IV as a direct manifestation of the canonical-vs-grand-canonical fluctuation mismatch.

The first  $1/\tau$  correction follows from extending the virial expansion (43) of  $f_\tau$  to next order. Recalling the virial decomposition (44) and the Gaussian moments (45), the high- $\tau$  form of  $g_0$  is given by (46) above, which we rewrite here in the compact form

$$g_0(u; \tau) = z^2 \frac{\pi}{2} \tau^2 e^{-2u^2/\tau} \left[ 1 - z \frac{3}{2^{3/2}} e^{-u^2/\tau} + \mathcal{O}(z^2) \right]. \quad (98)$$

The virial expansion of  $f_\tau(1 - f_\tau) = f_\tau - f_\tau^2 + \dots$  gives, in turn,

$$J_\alpha = I_\alpha - z \Delta_\alpha + \mathcal{O}(z^3), \quad K_\alpha = I_\alpha - 3z \Delta_\alpha + \mathcal{O}(z^3), \quad (99)$$

where  $\Delta_\alpha$  denotes the  $\mathcal{O}(z^2)$  piece of  $I_\alpha$  (i.e.  $\Delta_0 = G_2$ ,  $\Delta_2 = H_2$ ). The corresponding corrections to (93) read

$$\partial_t g_0 = 2g_0 - z^3 Y(u; \tau) + \mathcal{O}(z^4), \quad (100)$$

$$\partial_t^2 g_0 = 4g_0 - 5z^3 Y(u; \tau) + \mathcal{O}(z^4), \quad (101)$$

with  $Y(u; \tau) := G_1 H_2 + G_2 H_1 = (\pi/2) \tau^2 (3/2^{3/2}) e^{-3u^2/\tau}$ . Likewise, integrating (99) over  $u$ ,

$$V_2(\tau) = \pi\tau [z - z^2 + \mathcal{O}(z^3)], \quad V_3(\tau) = \pi\tau [z - 2z^2 + \mathcal{O}(z^3)], \quad (102)$$

so that  $V_3/V_2^2 = (\pi\tau z)^{-1}[1 + \mathcal{O}(z^2)]$  has no  $\mathcal{O}(z)$  correction (the corrections to  $V_3$  and  $V_2^2$  cancel at this order). Inserting (100)–(102) into (65) and integrating, then using the number constraint (49) ( $z = 1/\tau + 1/(2\tau^2) + \mathcal{O}(\tau^{-3})$ ), we obtain

$$B(\tau) = -\frac{\sqrt{\tau}}{\pi^{3/2}} \left[ 1 + \frac{5 - 3\sqrt{3}}{2} \frac{1}{\tau} + \mathcal{O}\left(\frac{1}{\tau^2}\right) \right], \quad (\tau \gg 1), \quad (103)$$

where the coefficient of the  $1/\tau$  term is negative, so this correction tempers the magnitude of  $B(\tau)$  relative to its leading Boltzmann form  $-\sqrt{\tau}/\pi^{3/2}$ .

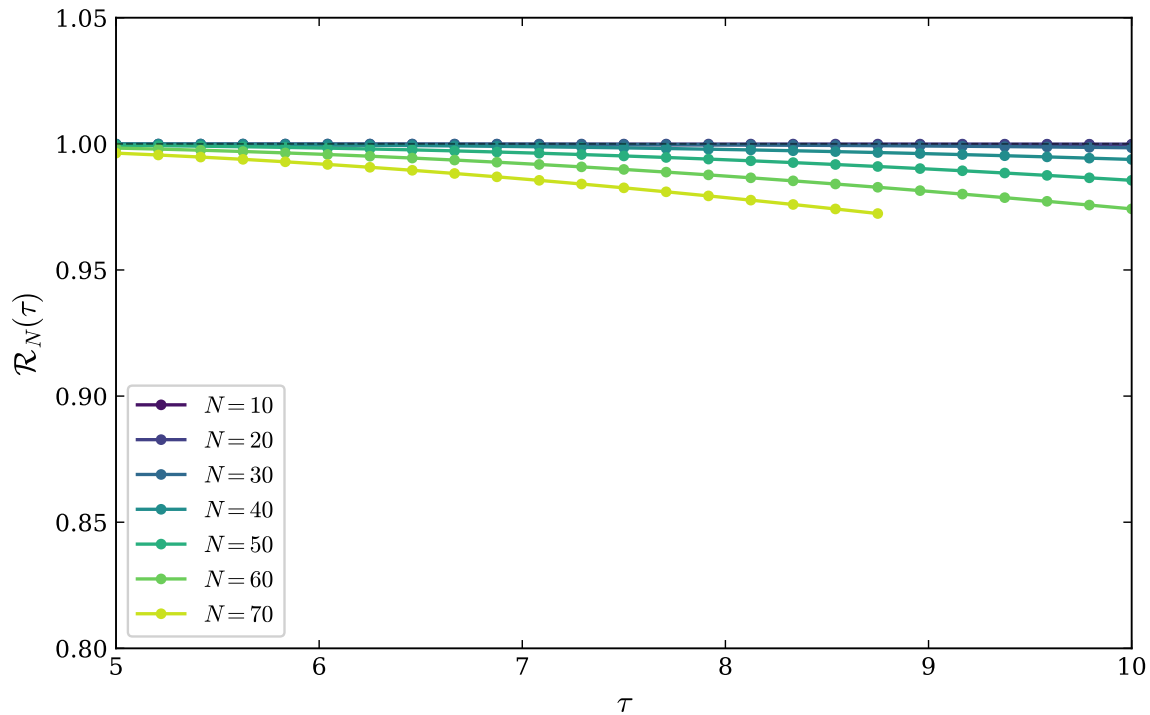


FIG. 3: High- $\tau$  verification of the canonical scaling law: the same ratio  $\mathcal{R}_N$  as in Fig. 2, now plotted on  $\tau \in [5, 10]$ .

The collapse onto unity (dashed line) confirms the asymptotic forms  $A(\tau) \simeq \sqrt{\tau}/\pi^{3/2}$  from (51) and  $B(\tau) \simeq -\sqrt{\tau}/\pi^{3/2}$  from (103) in the Boltzmann regime. Residual deviation from unity at the largest- $N$ , highest- $\tau$  corner is dominated by the spatial-integral truncation at finite  $M_{\max}$  and shrinks systematically with increasing  $M_{\max}$ .

### C. Numerical evaluation for intermediate $\tau$

In the intermediate regime  $\tau \sim 1$  no small parameter is available, so the scaling functions  $A(\tau)$  and  $B(\tau)$  must be computed numerically from their integral representations (32) and (67).

The procedure is straightforward in principle: for each  $u$ , we evaluate the six  $q$ -integrals (27), (58), (59); form  $g_0(u; \tau)$ ,  $\partial_t g_0(u; \tau)$  and  $\partial_t^2 g_0(u; \tau)$  via (60)–(61); and integrate in  $u$  to obtain  $A(\tau)$ ,  $V_2(\tau)$ ,  $V_3(\tau)$  and  $B(\tau)$  through (67). The Fermi factor is evaluated with the self-consistent  $\xi(\tau)$  from (26); all integrands decay exponentially at large argument, so truncating each integration domain at  $\sim \sqrt{\tau}$  times an  $\mathcal{O}(1)$  factor introduces only exponentially small deviation. The full quadrature scheme, convergence criteria, and a discussion of error control for the partial cancellations in  $\mathcal{H}(u; \tau)$  are documented in Appendix C.

To validate the universal-integral evaluation, we compute the canonical contact  $\mathcal{C}_N(\tau)$  by contour projection and check that (12) holds with coefficients consistent with (32) and (67). Concretely, for fixed  $\tau$  and a set of particle numbers  $N \in \{N_1, \dots, N_M\}$  we fit

$$\frac{\mathcal{C}_N(\tau)}{N^{5/2}} = A(\tau) + \frac{B(\tau)}{N} + \mathcal{O}(N^{-2}), \quad (104)$$

so that a linear regression of  $\mathcal{C}_N(\tau)/N^{5/2}$  against  $1/N$  returns  $A(\tau)$  as the intercept and  $B(\tau)$  as the slope. Agreement with the universal-integral values serves as a strong consistency check for both the scaling exponents and the numerical implementation. Compact closed-form Padé approximants  $A_P(\tau)$  and  $B_P(\tau)$ , valid uniformly on the reduced temperature range, are constructed in Appendix C — eqs. (C6) and (C10) — from analytic asymptotic constraints supplemented by a minimax fit. The scaling-law verification using both the numerical and the Padé scaling functions is shown in Fig. 4, and the resulting  $A(\tau)$  and  $B(\tau)$  are displayed in Fig. 5 together with their analytic Sommerfeld and virial limits.

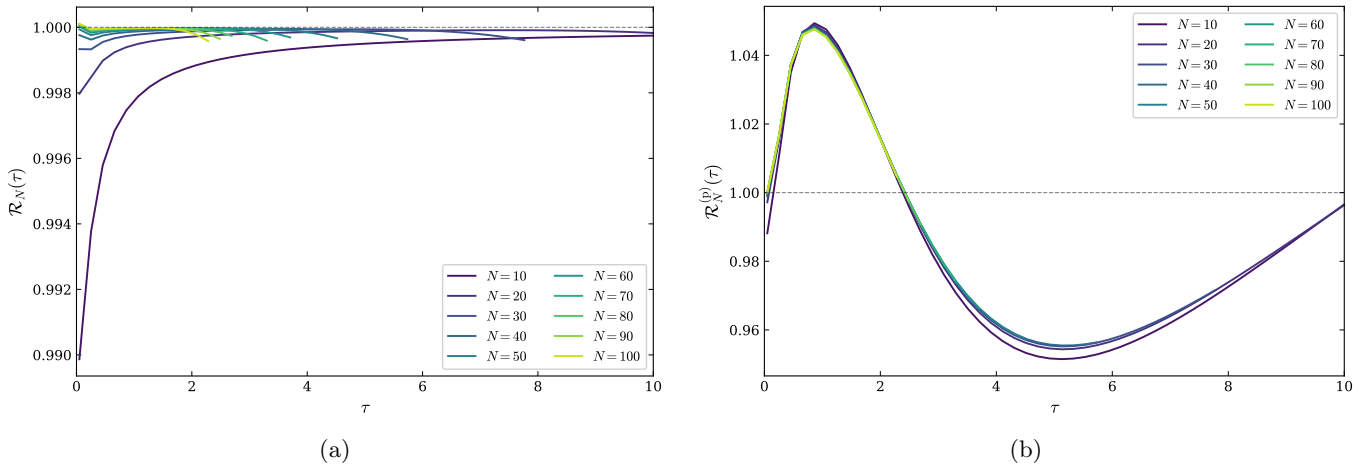


FIG. 4: Full- $\tau$  scaling verification of Eq. (12) across  $\tau \in [0, 10]$  and  $N = 10, \dots, 100$ . (a) Ratio  $\mathcal{R}_N$  from (68), evaluated with the numerical scaling functions  $A(\tau)$  and  $B(\tau)$ . (b) Ratio  $\mathcal{R}_N^{(P)}$  from (C14), evaluated with the Padé approximants  $A_P(\tau)$  and  $B_P(\tau)$  of (C6) and (C10). In both panels the curves collapse onto unity (dashed line), confirming the canonical scaling law from the degenerate ( $\tau \ll 1$ ) to the Boltzmann ( $\tau \gg 1$ ) regimes and the validity of the Padé approximants as closed-form substitutes for the universal integrals. Residual deviations at the smallest  $N$  reflect the genuine  $\mathcal{O}(N^{1/2})$  next-to-subleading correction.

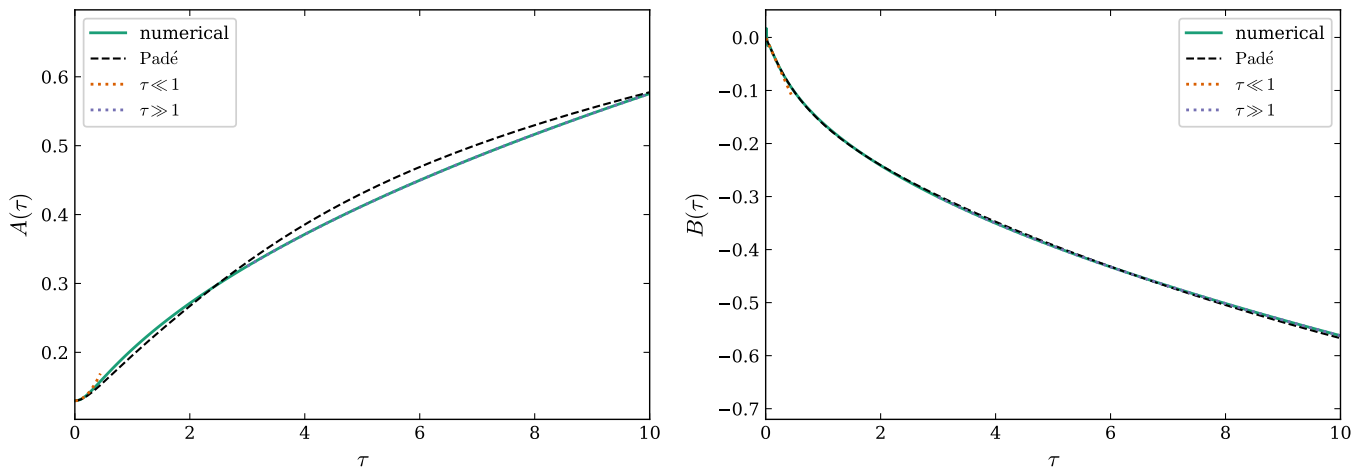


FIG. 5: Universal scaling functions  $A(\tau)$  (left panel) and  $B(\tau)$  (right panel). Solid blue: numerical evaluation of the integral representations (32) and (67) using the self-consistent  $\xi(\tau)$  from (26). Dashed black: Padé approximants (C6) and (C10). Dotted red: low- $\tau$  Sommerfeld expansions (39) and (91). Dotted green: high- $\tau$  virial expansions (51) and (103). The Padé approximants interpolate between the two asymptotic regimes over  $\tau \in [0, 10]$ .

#### IV. ENSEMBLE CORRESPONDENCE

The canonical analysis of Sec. III A–III B established the scaling law (12) through a contour-integral representation followed by saddle reduction. The same machinery, evaluated at the saddle alone, is essentially the grand-canonical calculation. Examining what survives—and what disappears—when the contour is removed clarifies the physical origin of the subleading coefficient  $B(\tau)$  as an ensemble-correspondence effect.

In the GCE the occupations  $\eta_m \in \{0, 1\}$  are independent Bernoulli variables with means  $\bar{n}_n(z) = (e^{\beta(\varepsilon_n - \mu)} + 1)^{-1}$  and joint moments  $\langle \eta_m \eta_n \rangle_{\text{GCE}} = \bar{n}_m \bar{n}_n$  for  $m \neq n$ . Inserting this factorisation into the pair representation of the integrand (cf. Appendix B) and using  $A_{nn}(x) := 0$  collapses the double sum to the same kernel functional that appears under the contour in (B18), but evaluated directly at the GCE fugacity  $z = e^{\beta\mu}$ :

$$F^{\text{GCE}}(x; z) = \rho_z(x) \kappa_z(x) - S_z(x)^2, \quad \mathcal{C}^{\text{GCE}} = \frac{2}{\pi} \int dx F^{\text{GCE}}(x; z), \quad (105)$$

with  $\rho_z, \kappa_z, S_z$  defined as in (11). No contour integration is required: the right-hand side of (105) is the GCE expectation.

To match  $\langle N \rangle_{\text{GCE}} = N$  we impose the same number condition (14) as the canonical saddle, which in the fixed- $\tau$  scaling limit (with  $\beta = 1/(\tau N)$  and  $\mu = \xi(\tau) N$ ) reduces to the self-consistent transcendental equation (26) already introduced in Sec. III A. The phase-space Fermi factor is the one in (25), evaluated with the self-consistent  $\xi(\tau)$ .

The LDA reduction of (105) is identical to that performed in Sec. III A; setting  $S_z := 0$  by parity and using the scaling variables (22),

$$F^{\text{GCE}}(x; z) = \frac{N^2}{\pi^2} g_0(u; \tau) + \mathcal{O}(1), \quad x = \sqrt{2N} u, \quad (106)$$

with  $g_0(u; \tau) = I_0(u; \tau) I_2(u; \tau)$  as in (56). The crucial difference with respect to the canonical decomposition (64) is the absence of the  $\mathcal{O}(N)$  saddle-fluctuation term: (105) contains no contour integral, and therefore no Gaussian fluctuations to expand around. Integrating (106) yields

$$\mathcal{C}_{\langle N \rangle = N}^{\text{GCE}}(\tau) = A(\tau) N^{5/2} + \mathcal{O}(N^{1/2}), \quad (107)$$

with the same  $A(\tau)$  as in (32), now understood with the self-consistent  $\xi(\tau)$ , and no  $N^{3/2}$  correction at the LDA order. The leading scaling function  $A(\tau)$  is therefore an ensemble-independent universal quantity.

It is important to distinguish two senses in which (107) holds. At the LDA level, the absence of  $N^{3/2}$  corrections is true by construction: the only  $N$ -dependence in  $F^{\text{GCE}}(x; z_*)$  enters through  $\sqrt{2N}$  in the rescaled coordinate and through the Fermi factor at the LDA-saddle fugacity, both of which produce only even powers of  $N^{1/2}$ .

Subtracting (107) from the canonical expansion (12) yields the central observation of this section,

$$\Delta\mathcal{C}(\tau) := \mathcal{C}_N^{\text{CE}}(\tau) - \mathcal{C}_{\langle N \rangle = N}^{\text{GCE}}(\tau) = B(\tau) N^{3/2} + \mathcal{O}(N^{1/2}), \quad (108)$$

with  $B(\tau)$  given explicitly by (67). Equation (108) provides the physical interpretation of the subleading scaling function:  $B(\tau) N^{3/2}$  is the ensemble correction to the contact—the part of  $\mathcal{C}_N^{\text{CE}}$  sourced by the constraint of fixed  $N$  and therefore absent from the GCE. Equivalently, the GCE delivers the leading  $A(\tau) N^{5/2}$  directly from the local kernel functional, while the CE pays the price of a fluctuation correction of magnitude exactly  $B(\tau) N^{3/2}$ .

The result (108) can be derived independently from the standard ensemble-correspondence formula (see e.g. the textbook discussion in [43] or the modern review of large-deviation methods in statistical mechanics [44]): for any extensive observable  $O$ ,

$$\langle O \rangle_{\text{CE}} - \langle O \rangle_{\text{GCE}} \simeq \frac{1}{2\kappa_2} \partial_N^2 \langle O \rangle_{\text{GCE}} - \frac{\kappa_3}{2\kappa_2^2} \partial_N \langle O \rangle_{\text{GCE}}, \quad (109)$$

with  $\kappa_2, \kappa_3$  the GCE particle-number cumulants. In the fixed- $\tau$  scaling limit, the cumulants reduce as in (62)–(63), exhibiting the global functions  $V_2, V_3$  as nothing more than rescaled particle-number cumulants of the GCE. Setting  $O = \mathcal{C}$  with  $\langle \mathcal{C} \rangle_{\text{GCE}} = A(\tau) N^{5/2}$ , each derivative drops a power of  $N$  while each  $1/\kappa$  factor restores  $1/N$ , so both terms in (109) contribute at order  $N^{3/2}$ . Reconstructing the coefficients with the explicit Wigner integrands recovers (67) term by term, and confirms that the structure of  $B(\tau)$ —a local part proportional to  $\partial_t^2 g_0/V_2$  and a global part proportional to  $V_3/V_2^2$ —is dictated by the curvature and skewness of the GCE particle-number distribution.

In the dilute Boltzmann regime  $\tau \gg 1$ , the GCE distribution of  $N$  becomes Poissonian,  $\kappa_2 \simeq \langle N \rangle$  and hence  $V_2(\tau) \rightarrow \pi$  as in (96). The ratio  $B/A$  then collapses to the universal value  $-1$  as in (97), in agreement with (103).

## V. CONCLUSIONS

We have derived the canonical-ensemble large- $N$  scaling law (12) of Tan's contact for the harmonically trapped Tonks–Girardeau gas at fixed reduced temperature. The leading coefficient  $A(\tau)$  coincides with the local-density-approximation result and reproduces the known zero-temperature value  $A(0) = 128\sqrt{2}/(45\pi^3)$ . The subleading coefficient  $B(\tau)$ , the central new object of this work, admits a universal first-principles representation (67) in terms of phase-space integrals of the Fermi factor, has explicit Sommerfeld and virial limits given in (91) and (103), and is identified through (108) with the canonical-versus-grand-canonical ensemble difference at fixed mean particle number. In the Boltzmann limit, the universal asymptotic coefficient ratio  $B/A \rightarrow -1$  — equivalently  $B(\tau \gg 1) \simeq -A(\tau)$  — emerges from the Poissonian particle-number statistics of the GCE: the canonical contact lies below the corresponding grand-canonical contact at the canonical-saddle fugacity, with the relative correction  $|B/A|/N = 1/N$  in the dilute classical regime. We construct compact closed-form Padé approximants for  $A(\tau)$  and  $B(\tau)$ , valid uniformly on  $\tau \in [0, 10]$ , and the scaling law is verified numerically against canonical contour-integration data for  $N$  up to 100 across the full temperature range.

The expansion derived in this manuscript is for fixed positive  $\tau$  followed by  $N \rightarrow \infty$ . The strictly zero-temperature limit ( $\tau = 0$ ) has a qualitatively different finite- $N$  hierarchy: the thermal Fermi-surface smearing that broadens the turning-point layer to width  $\tau$  collapses to the Airy width  $N^{-2/3}$ , and the resulting edge corrections produce distinct  $N^{3/4}$  and  $N^{1/4}$  contributions [33, 38]. Since (85) vanishes linearly as  $\tau \rightarrow 0$ , the  $N^{3/2}$  term derived here becomes subdominant to the zero-temperature edge corrections in the strict  $\tau \rightarrow 0$  limit, and the two limits do not commute. The crossover between the two regimes occurs at  $\tau \sim N^{-2/3}$ , where the thermal width matches the Airy width. The present analysis is valid for  $\tau \gg N^{-2/3}$ , which at  $N = 100$  corresponds to  $\tau \gtrsim 0.05$ .

The result extends the canonical analysis of Ref. [39] to many particles through the kernel representation and identifies the precise origin of the subleading  $N^{3/2}$  term as a finite- $N$  ensemble-correspondence effect. In light of recent direct contact measurements in trapped one-dimensional Bose gases [28], the explicit scaling functions  $A(\tau)$  and  $B(\tau)$  provide a quantitative target against which finite-temperature trapped-geometry data can be compared.

Several extensions are natural. The boundary-layer (Airy) corrections to the contact, which produce additional subleading terms scaling as  $N^{3/4}$  and  $N^{1/4}$  at zero temperature [38], persist at finite temperature but are expected to be exponentially suppressed by the thermal smoothing of the Fermi surface; their explicit finite- $T$  form is the natural sequel to the present work. The same contour-integral framework can also be applied to multi-component fermionic mixtures [36, 37] and to the trapped Lieb–Liniger gas at finite coupling [34], where similar canonical-vs-grand-canonical distinctions are expected to control the subleading scaling.

## DATA AVAILABILITY

The numerical data and code that support the findings of this study are available at [github.com/ftahas/Contact\\_Scaling](https://github.com/ftahas/Contact_Scaling).

## Appendix A: Derivation of the contact

We start with the  $j$ -body density matrix of  $N$  particles at temperature  $T$ ,

$$\begin{aligned} \varrho^{(j)}(x_1, \dots, x_j; x'_1, \dots, x'_j) &= \frac{N!}{(N-j)!} Z^{-1} \sum_{\alpha} e^{-\beta E_{\alpha}} \int dx_{j+1} \dots dx_N \Psi_{\alpha}^{(b)*}(x_1, \dots, x_N) \\ &\times \Psi_{\alpha}^{(b)}(x'_1, \dots, x'_j, x_{j+1}, \dots, x_N), \end{aligned} \quad (\text{A1})$$

where  $Z = \sum_{\alpha} e^{-\beta E_{\alpha}}$  is the partition function and the system's total energy is simply the summation of all the individual single-particle energies, *i.e.*,  $E_{\alpha} = \sum_{i=1}^N \varepsilon_{n_i}$ , with  $\varepsilon_{n_i} = (n_i + 1/2)\hbar\omega$ . Invoking the Bose–Fermi mapping

$$\Psi_{\alpha}^{(b)}(x_1, \dots, x_N) = \Theta(x_1, \dots, x_N) \Psi_{\alpha}^{(f)}(x_1, \dots, x_N), \quad (\text{A2})$$

where  $\Theta(x_1, \dots, x_N) := \prod_{i < j} \text{sgn}(x_i - x_j)$  is either  $+1$  or  $-1$ , in order to compensate the anti-symmetrization of the fermionic wave function  $\Psi_{\alpha}^{(f)}$ , and  $\alpha$  is the quantum number describing the particles in a respective set of individual quantum numbers  $\{n_1, n_2, \dots, n_N\}$ , and the fermionic many-body wave function is given by the Slater determinant

$$\Psi_{\alpha}^{(f)}(x_1, \dots, x_N) = (N!)^{-1/2} \det[\phi_{n_i}(x_j)]_{n_i \in \{n_1, \dots, n_N\}; x_j \in \{x_1, \dots, x_N\}}, \quad (\text{A3})$$

with  $\phi_n(x)$  being the solutions of the harmonic oscillator single-particle solutions, eq. (A1) reads

$$\begin{aligned} \varrho^{(j)}(x_1, \dots, x_j; x'_1, \dots, x'_j) &= \frac{N!}{(N-j)!} Z^{-1} \sum_{\alpha} e^{-\beta E_{\alpha}} \int dx_{j+1} \dots dx_N \Theta(x_1, \dots, x_N) \\ &\times \Psi_{\alpha}^{(f)}(x_1, \dots, x_N) \Theta(x'_1, \dots, x'_j, x_{j+1}, \dots, x_N) \Psi_{\alpha}^{(f)}(x'_1, \dots, x'_j, x_{j+1}, \dots, x_N). \end{aligned} \quad (\text{A4})$$

Now we turn our focus to the integrand. It is possible to rewrite the product of the  $\Theta$ 's as

$$\begin{aligned} \Theta(x_1, \dots, x_N) \Theta(x'_1, \dots, x'_j, x_{j+1}, \dots, x_N) &= \Theta(x_1, \dots, x_j) \Theta(x'_1, \dots, x'_j) \\ &\times \prod_{i=j+1}^N \prod_{l=1}^{2j} \text{sgn}(x_i - y_l), \end{aligned} \quad (\text{A5})$$

with  $y_1 = x_1 < y_2 = x_2 < \dots < y_j = x_j < y_{j+1} = x'_1 < \dots < y_{2j} = x'_j$ . Now let us consider the set  $\mathfrak{S} = \{(y_1, y_2) \cup (y_3, y_4) \cup \dots \cup (y_{2j-1}, y_{2j})\}$ . It is straightforward to observe that

$$\prod_{i=1}^{2j} \text{sgn}(x - y_i) = \begin{cases} -1, & x \in \mathfrak{S} \\ +1, & x \notin \mathfrak{S} \end{cases}. \quad (\text{A6})$$

Denoting the number of variables among  $x_{j+1}, \dots, x_N$  which are in  $\mathfrak{S}$  by  $M_{\mathfrak{S}}$ , we have that

$$\Theta(x_1, \dots, x_N) \Theta(x'_1, \dots, x'_j, x_{j+1}, \dots, x_N) = \Theta(x_1, \dots, x_j) \Theta(x'_1, \dots, x'_j) (-1)^{M_{\mathfrak{S}}}. \quad (\text{A7})$$

Consequently, eq. (A4) results in

$$\begin{aligned} \varrho^{(j)}(x_1, \dots, x_j; x'_1, \dots, x'_j) &= \frac{N!}{(N-j)!} Z^{-1} \Theta(x_1, \dots, x_j) \Theta(x'_1, \dots, x'_j) \sum_{\alpha} e^{-\beta E_{\alpha}} \\ &\times \int dx_{j+1} \dots dx_N (-1)^{M_{\mathfrak{S}}} \Psi_{\alpha}^{(f)}(x_1, \dots, x_N) \Psi_{\alpha}^{(f)}(x'_1, \dots, x'_j, x_{j+1}, \dots, x_N). \end{aligned} \quad (\text{A8})$$

Now, considering any integral of the form

$$I = \int dx_1 \dots \int (-1)^{M_{\mathfrak{S}}} f(x_1, \dots, x_j), \quad (\text{A9})$$

where  $M_{\mathfrak{S}}$  is the number of integration variables inside the subdomain  $\mathfrak{S}$  and  $f$  is a symmetric function, it is possible to write

$$I = \sum_{m=0}^j \binom{j}{m} (-1)^m \int_{\mathfrak{S}} dx_1 \dots dx_m \int_{\text{Re}-\mathfrak{S}} dx_{m+1} \dots dx_j f(x_1, \dots, x_j). \quad (\text{A10})$$

Making use of  $\int_{\text{Re}-\mathfrak{S}} dx = \int_{\text{Re}} dx - \int_{\mathfrak{S}} dx$ , we have

$$I = \sum_{m=0}^j \binom{j}{m} (-1)^m \sum_{n=0}^{j-m} \binom{j-m}{n} (-1)^n \int_{\mathfrak{S}} dx_1 \dots dx_{m+n} \int_{\text{Re}} dx_{m+n+1} \dots dx_j f(x_1, \dots, x_j). \quad (\text{A11})$$

Performing the summation for  $m+n=i$ , (A11) reduces to

$$I = \sum_{i=0}^j \binom{j}{i} (-2)^i \int_{\mathfrak{S}} dx_1 \dots dx_i \int dx_{i+1} \dots dx_j f(x_1, \dots, x_j). \quad (\text{A12})$$

Thence, we have that the  $j$ -body density matrix (A8) can be written as

$$\begin{aligned} \varrho^{(j)}(x_1, \dots, x_j; x'_1, \dots, x'_j) &= \frac{N!}{(N-j)!} Z^{-1} \Theta(x_1, \dots, x_j) \Theta(x'_1, \dots, x'_j) \sum_{\alpha} e^{-\beta E_{\alpha}} \\ &\times \sum_{i=0}^{N-j} \binom{N-j}{i} (-2)^i \int_{\mathfrak{S}} dx_{j+1} \dots dx_{j+i} \int dx_{j+i+1} \dots dx_N \\ &\times \Psi_{\alpha}^{(f)}(x_1, \dots, x_N) \Psi_{\alpha}^{(f)}(x'_1, \dots, x'_j, x_{j+1}, \dots, x_N). \end{aligned} \quad (\text{A13})$$

The one-body density matrix gives the Lenard series

$$\begin{aligned} \varrho^{(1)}(x, x') &= \frac{N}{Z} \sum_{\alpha} e^{-\beta E_{\alpha}} \sum_{j=1}^{N-1} \binom{N-1}{j} (-2)^j [\text{sgn}(x-x')]^j \int_x^{x'} dx_2 \dots dx_{j+1} \\ &\times \int dx_{j+2} \dots dx_N \Psi_{\alpha}^{(f)}(x, x_2, \dots, x_N) \Psi_{\alpha}^{(f)}(x', x_2, \dots, x_N). \end{aligned} \quad (\text{A14})$$

The sum runs from  $j = 1$  rather than  $j = 0$ : the  $j = 0$  term would give the noninteracting fermionic one-body density matrix  $\varrho_f^{(1)}(x, x')$ , which is analytic in  $x' - x$  at short distances and therefore contributes neither to the universal  $|x' - x|^3$  behaviour nor to the  $k^{-4}$  tail of the momentum distribution. The contact is sourced entirely by the non-analytic  $|x' - x|^3$  piece of  $\varrho^{(1)}$ , generated by the  $[\text{sgn}(x - x')]^j$  factors at  $j \geq 1$ . Here it is possible to recognize the  $j$ -body fermionic correlator as

$$\varrho^{(1)}(x, x') = \sum_{j=1}^{N-1} \frac{(-2)^j}{j!} [\text{sgn}(x - x')]^j \int_x^{x'} dx_2 \dots dx_{j+1} \varrho_f^{(j+1)}(x, x_2, \dots, x_{j+1}; x', x_2, \dots, x_{j+1}), \quad (\text{A15})$$

where

$$\begin{aligned} \varrho_f^{(j)}(x_1, \dots, x_j; x'_1, \dots, x'_j) &= \frac{N!}{(N-j)!} Z^{-1} \sum_{\alpha} e^{-\beta E_{\alpha}} \\ &\times \int dx_{j+1} \dots dx_N \Psi_{\alpha}^{(f)}(x_1, \dots, x_N) \Psi_{\alpha}^{(f)}(x'_1, \dots, x'_j, x_{j+1}, \dots, x_N). \end{aligned} \quad (\text{A16})$$

As we are interested in the contact, we are going to restrict ourselves to small distances,  $|x' - x| \ll 1$ . Therefore, we consider only the term  $j = 1$ , because the terms  $j > 1$  produce negligible results in the small distance approximation:

$$\begin{aligned} \varrho^{(1)}(x, x') &\underset{x \rightarrow x'}{\sim} 2 \text{sgn}(x' - x) \int_x^{x'} dx_2 \varrho_f^{(2)}(x, x_2; x', x_2) \\ &\approx 2 \text{sgn}(x' - x) \varrho_f^{(2)}(x, R; x', R) \delta x, \end{aligned} \quad (\text{A17})$$

where  $R := (x + x')/2$  and  $\delta x := x' - x$ .

Now we proceed with the explicit evaluation of  $\varrho^{(2)}$  making use of (A16) together with (A3).

*N=2 particles*

$$\begin{aligned} \varrho_f^{(2)}(x, R; x', R) &= Z^{-1} \sum_{n_1, n_2} e^{-\beta(\varepsilon_{n_1} + \varepsilon_{n_2})} \begin{vmatrix} \phi_{n_1}(x) & \phi_{n_2}(x) \\ \phi_{n_1}(R) & \phi_{n_2}(R) \end{vmatrix} \begin{vmatrix} \phi_{n_1}(x') & \phi_{n_2}(x') \\ \phi_{n_1}(R) & \phi_{n_2}(R) \end{vmatrix} \\ &= Z^{-1} \sum_{n_1, n_2} e^{-\beta(\varepsilon_{n_1} + \varepsilon_{n_2})} [\phi_{n_1}(R - \delta x/2) \phi_{n_2}(R) - \phi_{n_2}(R - \delta x/2) \phi_{n_1}(R)] \\ &\quad \times [\phi_{n_1}(R + \delta x/2) \phi_{n_2}(R) - \phi_{n_2}(R + \delta x/2) \phi_{n_1}(R)] \\ &= Z^{-1} \sum_{n_1, n_2} e^{-\beta(\varepsilon_{n_1} + \varepsilon_{n_2})} \left[ \left( \phi_{n_1} - \frac{\delta x}{2} \partial_R \phi_{n_1} \right) \phi_{n_2} - \left( \phi_{n_2} - \frac{\delta x}{2} \partial_R \phi_{n_2} \right) \phi_{n_1} \right] \\ &\quad \times \left[ \left( \phi_{n_1} + \frac{\delta x}{2} \partial_R \phi_{n_1} \right) \phi_{n_2} - \left( \phi_{n_2} + \frac{\delta x}{2} \partial_R \phi_{n_2} \right) \phi_{n_1} \right] \\ &= Z^{-1} \sum_{n_1, n_2} e^{-\beta(\varepsilon_{n_1} + \varepsilon_{n_2})} \frac{\delta x^2}{4} \\ &\quad \times [(\phi_{n_2} \partial_R \phi_{n_1})^2 + (\phi_{n_1} \partial_R \phi_{n_2})^2 - 2\phi_{n_1} \phi_{n_2} \partial_R \phi_{n_1} \partial_R \phi_{n_2}]. \end{aligned} \quad (\text{A18})$$

$N=3$  particles

$$\begin{aligned}
\rho_f^{(2)}(x, R; x', R) &= Z^{-1} \sum_{n_1, n_2, n_3} e^{-\beta(\varepsilon_{n_1} + \varepsilon_{n_2} + \varepsilon_{n_3})} \\
&\times \int dx_3 \begin{vmatrix} \phi_{n_1}(x) & \phi_{n_2}(x) & \phi_{n_3}(x) \\ \phi_{n_1}(R) & \phi_{n_2}(R) & \phi_{n_3}(R) \\ \phi_{n_1}(x_3) & \phi_{n_2}(x_3) & \phi_{n_3}(x_3) \end{vmatrix} \begin{vmatrix} \phi_{n_1}(x') & \phi_{n_2}(x') & \phi_{n_3}(x') \\ \phi_{n_1}(R) & \phi_{n_2}(R) & \phi_{n_3}(R) \\ \phi_{n_1}(x_3) & \phi_{n_2}(x_3) & \phi_{n_3}(x_3) \end{vmatrix} \\
&= Z^{-1} \sum_{n_1, n_2, n_3} e^{-\beta(\varepsilon_{n_1} + \varepsilon_{n_2} + \varepsilon_{n_3})} \left[ \phi_{n_1}^2 \left( \frac{\delta x}{2} \partial_R \phi_{n_2} \right)^2 + \phi_{n_1}^2 \left( \frac{\delta x}{2} \partial_R \phi_{n_3} \right)^2 \right. \\
&+ \phi_{n_2}^2 \left( \frac{\delta x}{2} \partial_R \phi_{n_1} \right)^2 + \phi_{n_2}^2 \left( \frac{\delta x}{2} \partial_R \phi_{n_3} \right)^2 + \phi_{n_3}^2 \left( \frac{\delta x}{2} \partial_R \phi_{n_1} \right)^2 \\
&+ \phi_{n_3}^2 \left( \frac{\delta x}{2} \partial_R \phi_{n_2} \right)^2 - 2\phi_{n_1} \phi_{n_2} \frac{\delta x^2}{4} \partial_R \phi_{n_1} \partial_R \phi_{n_2} \\
&\left. - 2\phi_{n_1} \phi_{n_3} \frac{\delta x^2}{4} \partial_R \phi_{n_1} \partial_R \phi_{n_3} - 2\phi_{n_2} \phi_{n_3} \frac{\delta x^2}{4} \partial_R \phi_{n_2} \partial_R \phi_{n_3} \right]. \tag{A19}
\end{aligned}$$

In the steps above we have used the differentiation relation

$$\partial_R \phi(R) = \frac{\phi(R) - \phi(R - \delta x/2)}{\delta x/2}, \tag{A20}$$

and the orthogonality of the  $\phi$ 's

$$\int_{-\infty}^{+\infty} dx \phi_m(x) \phi_n(x) = \delta_{m,n}. \tag{A21}$$

Therefore, from the explicit evaluations for  $N = 2$  and  $3$  particles, we can generalize the fermionic two-body density matrix for  $N$  particles as

$$\begin{aligned}
\rho_f^{(2)}(x, R; x', R) &= \frac{(x' - x)^2}{4} Z^{-1} \sum_{n_1, n_2, \dots, n_N} e^{-\beta \sum_{i=1}^N \varepsilon_{n_i}} \\
&\times \sum_{j \neq k} \left\{ [\phi_{n_j}(R) \partial_R \phi_{n_k}(R)]^2 - \phi_{n_j}(R) \phi_{n_k}(R) \partial_R \phi_{n_j}(R) \partial_R \phi_{n_k}(R) \right\}. \tag{A22}
\end{aligned}$$

Consequently, we have

$$\rho^{(1)}(x, x') \approx \frac{|x' - x|^3}{3} F(R), \tag{A23}$$

with the definition

$$F(R) := Z^{-1} \sum_{n_1, \dots, n_N} e^{-\beta \sum_{i=1}^N \varepsilon_{n_i}} \sum_{j \neq k} \left\{ [\phi_{n_j}(R) \partial_R \phi_{n_k}(R)]^2 - \phi_{n_j}(R) \phi_{n_k}(R) \partial_R \phi_{n_j}(R) \partial_R \phi_{n_k}(R) \right\}. \tag{A24}$$

Now we will use our analysis of the one-body density matrix in order to inspect the momentum distribution

$$n(k) = \frac{1}{2\pi} \int_{-\infty}^{\infty} dx \int_{-\infty}^{\infty} dx' e^{ik(x-x')} \rho^{(1)}(x, x'). \tag{A25}$$

Let

$$R = \frac{x + x'}{2}, \quad s = x - x', \quad dx dx' = dR ds,$$

so that

$$n(k) = \frac{1}{2\pi} \int_{-\infty}^{\infty} dR \int_{-\infty}^{\infty} ds e^{iks} \rho^{(1)}\left(R + \frac{s}{2}, R - \frac{s}{2}\right). \tag{A26}$$

The short-distance condition,  $|s| \rightarrow 0$ , gives

$$\rho^{(1)}\left(R + \frac{s}{2}, R - \frac{s}{2}\right) \simeq \frac{|s|^3}{3} F(R).$$

Hence, for large  $|k|$ ,

$$n(k) \simeq \frac{1}{2\pi} \int dR \frac{F(R)}{3} \int_{-\infty}^{\infty} ds e^{iks} |s|^3. \quad (\text{A27})$$

Now we make use of the asymptotic behaviour of the Fourier transform of  $|x - x_0|^{a-1} f(x)$ ,

$$\int dx e^{-ik(x-x_0)} |x - x_0|^{a-1} f(x) = \frac{2}{k^a} f(x_0) \cos\left(\frac{\pi a}{2}\right) \Gamma(a). \quad (\text{A28})$$

Taking  $a = 4$ ,  $f := 1$ ,  $x_0 = 0$ , we get

$$\int_{-\infty}^{\infty} ds e^{iks} |s|^3 = \frac{2}{k^4} \cos(2\pi) \Gamma(4) = \frac{12}{k^4}. \quad (\text{A29})$$

Therefore,

$$n(k) \simeq \frac{1}{2\pi} \int dR \frac{F(R)}{3} \frac{12}{k^4} = \frac{2}{\pi} \frac{1}{k^4} \int_{-\infty}^{\infty} dR F(R). \quad (\text{A30})$$

Finally, with  $\mathcal{C} = \lim_{k \rightarrow \infty} k^4 n(k)$ ,

$$\mathcal{C} = \frac{2}{\pi} \int_{-\infty}^{\infty} dR F(R). \quad (\text{A31})$$

## Appendix B: Kernel representation

Here we derive the kernel representation for the contact. For that, we work with our integrand

$$F_N(x) := Z_N^{-1} \sum_{n_1 < \dots < n_N} e^{-\beta \sum_{i=1}^N \varepsilon_{n_i}} \sum_{j \neq k} \left\{ [\phi_{n_j}(x) \partial_x \phi_{n_k}(x)]^2 - \phi_{n_j}(x) \phi_{n_k}(x) \partial_x \phi_{n_j}(x) \partial_x \phi_{n_k}(x) \right\}, \quad (\text{B1})$$

with the canonical partition function

$$Z_N = \sum_{n_1 < \dots < n_N} \exp\left(-\beta \sum_{i=1}^N \varepsilon_{n_i}\right). \quad (\text{B2})$$

We start by rewriting the canonical sum using occupation variables. For that, let us introduce occupation numbers  $\eta_n \in \{0, 1\}$  with the fixed- $N$  constraint

$$\sum_{n=0}^{\infty} \eta_n = N, \quad E[\eta] = \sum_{n=0}^{\infty} \eta_n \varepsilon_n. \quad (\text{B3})$$

Then the canonical partition function becomes

$$Z_N = \sum_{\{\eta\}} e^{-\beta E[\eta]} \delta_{\sum_n \eta_n, N}, \quad (\text{B4})$$

and the sum over occupied levels can be rewritten as

$$\sum_{j \neq k} (\dots) = \sum_{m \neq n} \eta_m \eta_n (\dots)_{m,n},$$

where  $(\dots)_{m,n}$  means: replace  $(n_j, n_k)$  by  $(m, n)$ . We define the symmetric kernel-like building block

$$A_{mn}(x) := [\phi_m(x)\phi'_n(x)]^2 - \phi_m(x)\phi_n(x)\phi'_m(x)\phi'_n(x). \quad (\text{B5})$$

Then (B1) becomes

$$F_N(x) = \sum_{m \neq n} \langle \eta_m \eta_n \rangle_N A_{mn}(x), \quad (\text{B6})$$

with the canonical expectation

$$\langle \mathcal{O}(\eta) \rangle_N := \frac{1}{Z_N} \sum_{\{\eta\}} e^{-\beta E[\eta]} \delta_{\sum_n \eta_n, N} \mathcal{O}(\eta). \quad (\text{B7})$$

Note that we could also include the  $m = n$  terms in (B6) since  $A_{nn}(x) = 0$  identically.

The grand partition function  $\Xi(z)$  is defined in (7), with the canonical  $Z_N$  recovered through the contour representation (8). Similarly, for any function of occupations  $\mathcal{O}(\eta)$ ,

$$\sum_{\{\eta\}} e^{-\beta E[\eta]} \delta_{\sum_n \eta_n, N} \mathcal{O}(\eta) = \frac{1}{2\pi i} \oint_{\mathcal{C}} \frac{dz}{z^{N+1}} \sum_{\{\eta\}} e^{-\beta E[\eta]} z^{\sum_n \eta_n} \mathcal{O}(\eta). \quad (\text{B8})$$

Now, for fixed  $z$ , the occupations are independent Bernoulli random variables with

$$\mathbb{P}_z(\eta_n = 1) = f_n(z), \quad f_n(z) := \frac{ze^{-\beta \varepsilon_n}}{1 + ze^{-\beta \varepsilon_n}}.$$

Equivalently, for fixed  $z$ ,

$$\sum_{\{\eta\}} e^{-\beta E[\eta]} z^{\sum \eta} = \Xi(z), \quad \sum_{\{\eta\}} e^{-\beta E[\eta]} z^{\sum \eta} \eta_m \eta_n = \Xi(z) f_m(z) f_n(z) \quad (m \neq n). \quad (\text{B9})$$

Therefore, for  $m \neq n$ ,

$$\langle \eta_m \eta_n \rangle_N = \frac{1}{Z_N} \frac{1}{2\pi i} \oint_{\mathcal{C}} \frac{dz}{z^{N+1}} \Xi(z) f_m(z) f_n(z). \quad (\text{B10})$$

Plugging (B10) into (B6) yields an exact contour representation:

$$\begin{aligned} F_N(x) &= \sum_{m \neq n} A_{mn}(x) \frac{1}{Z_N} \frac{1}{2\pi i} \oint_{\mathcal{C}} \frac{dz}{z^{N+1}} \Xi(z) f_m(z) f_n(z) \\ &= \frac{1}{Z_N} \frac{1}{2\pi i} \oint_{\mathcal{C}} \frac{dz}{z^{N+1}} \Xi(z) \sum_{m \neq n} f_m(z) f_n(z) A_{mn}(x). \end{aligned} \quad (\text{B11})$$

The final step is to define the  $z$ -kernel

$$K_z(x, y) := \sum_{n=0}^{\infty} f_n(z) \phi_n(x) \phi_n(y), \quad (\text{B12})$$

together with its associated local quantities

$$\rho_z(x) := K_z(x, x) = \sum_{n \geq 0} f_n(z) \phi_n(x)^2, \quad (\text{B13})$$

$$S_z(x) := \partial_y K_z(x, y) \Big|_{y=x} = \sum_{n \geq 0} f_n(z) \phi_n(x) \phi'_n(x), \quad (\text{B14})$$

$$\kappa_z(x) := \partial_x \partial_y K_z(x, y) \Big|_{y=x} = \sum_{n \geq 0} f_n(z) \phi'_n(x)^2. \quad (\text{B15})$$

Expanding  $\rho_z \kappa_z - S_z^2$ :

$$\begin{aligned} \rho_z(x) \kappa_z(x) - S_z(x)^2 &= \sum_{m,n \geq 0} f_m(z) f_n(z) [\phi_m(x)^2 \phi_n'(x)^2 - \phi_m(x) \phi_m'(x) \phi_n(x) \phi_n'(x)] \\ &= \sum_{m,n \geq 0} f_m(z) f_n(z) A_{mn}(x). \end{aligned} \quad (\text{B16})$$

But  $A_{nn}(x) = 0$ , so

$$\sum_{m \neq n} f_m(z) f_n(z) A_{mn}(x) = \rho_z(x) \kappa_z(x) - S_z(x)^2. \quad (\text{B17})$$

Therefore, the inner sum in (B11) collapses to a kernel functional:

$$F_N(x) = \frac{1}{Z_N} \frac{1}{2\pi i} \oint_{\mathcal{C}} \frac{dz}{z^{N+1}} \Xi(z) [\rho_z(x) \kappa_z(x) - S_z(x)^2]. \quad (\text{B18})$$

Equivalently, entirely in terms of  $K_z$ ,

$$F_N(x) = \frac{1}{Z_N} \frac{1}{2\pi i} \oint_{\mathcal{C}} \frac{dz}{z^{N+1}} \Xi(z) \left[ K_z(x, x) \partial_x \partial_y K_z(x, y) \Big|_{y=x} - \left( \partial_y K_z(x, y) \Big|_{y=x} \right)^2 \right]. \quad (\text{B19})$$

### 1. Pair representation

For a fixed Slater determinant built from orbitals  $\{n_1, \dots, n_N\}$ , define the configuration kernel

$$K_{\text{config}}(x, y) = \sum_{a: n_a=1} \phi_a(x) \phi_a(y), \quad (\text{B20})$$

and the local quantities

$$\rho = K(x, x), \quad S = \partial_y K(x, y) \Big|_{y=x}, \quad \kappa = \partial_x \partial_y K(x, y) \Big|_{y=x}. \quad (\text{B21})$$

For any set of occupation numbers  $\{n_a\} \in \{0, 1\}$ ,

$$\sum_{j \neq k} A_{n_j, n_k} = \rho_{\text{config}} \kappa_{\text{config}} - S_{\text{config}}^2, \quad (\text{B22})$$

where  $A_{a,b} = (\phi_a \phi_b')^2 - \phi_a \phi_b \phi_a' \phi_b'$ . Expanding the right-hand side we have

$$\rho \kappa - S^2 = \left( \sum_a n_a \phi_a^2 \right) \left( \sum_b n_b (\phi_b')^2 \right) - \left( \sum_a n_a \phi_a \phi_a' \right)^2 \quad (\text{B23})$$

$$= \sum_{a,b} n_a n_b [\phi_a^2 (\phi_b')^2 - \phi_a \phi_a' \phi_b \phi_b'] \quad (\text{B24})$$

$$= \sum_{a,b} n_a n_b A_{a,b}(x). \quad (\text{B25})$$

Since  $A_{a,a} = \phi_a^2 (\phi_a')^2 - \phi_a^2 (\phi_a')^2 = 0$ , the diagonal terms vanish and the double sum reduces to  $\sum_{a \neq b} n_a n_b A_{a,b}$ .

Symmetrising,  $A_{a,b} + A_{b,a} = (\phi_a \phi_b' - \phi_b \phi_a')^2$ , so the contribution from each unordered pair  $(a, b)$  with  $a < b$  is the squared Wronskian. Defining the pair integral

$$J_{ab} = \int dx (\phi_a \phi_b' - \phi_b \phi_a')^2. \quad (\text{B26})$$

Averaging (B22) over the canonical ensemble,

$$C_N^{\text{CE}} = \frac{2}{\pi} \sum_{a < b} \langle n_a n_b \rangle_{\text{CE}} J_{ab}. \quad (\text{B27})$$

If levels are statistically independent (as in the GCE), then for  $a \neq b$ ,  $\langle n_a n_b \rangle_{\text{GCE}} = \bar{n}_a \bar{n}_b$  where  $\bar{n}_a = (1 + e^{\beta(\varepsilon_a - \mu)})^{-1}$ . The contact takes the kernel form

$$\mathcal{C}_N^{\text{GCE}} = \frac{1}{\pi} \bar{\mathbf{n}}^T J \bar{\mathbf{n}}. \quad (\text{B28})$$

The fixed- $N$  constraint introduces correlations:

$$\langle n_a n_b \rangle_{\text{CE}} = \bar{n}_a^{\text{CE}} \bar{n}_b^{\text{CE}} + \text{Cov}_{\text{CE}}(n_a, n_b). \quad (\text{B29})$$

The covariance is negative (anti-bunching from the particle-number constraint) and scales as  $\text{Cov}_{\text{CE}}(n_a, n_b) \sim -\bar{n}_a(1 - \bar{n}_a) \bar{n}_b(1 - \bar{n}_b) / \text{Var}_{\text{GCE}}(N)$ . At finite  $\tau$ , the total ensemble difference  $\Delta \mathcal{C} := \mathcal{C}_N^{\text{CE}} - \mathcal{C}_N^{\text{GCE}}$  scales as  $\sim N^{3/2}$ , and therefore cannot be neglected at subleading order.

An exact canonical computation that avoids enumerating all  $\binom{M}{N}$  configurations uses the fugacity contour integral. Define the grand partition function  $\Xi(z) = \prod_{n=0}^{M-1} (1 + z q_n)$  with  $q_n = e^{-\beta \varepsilon_n}$ , and the fugacity-dependent occupation  $\bar{n}_a(z) = z q_a / (1 + z q_a)$ . Then

$$\mathcal{C}_N^{\text{CE}} = \frac{2}{\pi} \frac{1}{Z_N} \frac{1}{2\pi i} \oint \frac{dz}{z^{N+1}} \Xi(z) G(z), \quad (\text{B30})$$

where

$$G(z) = \sum_{a,b} \bar{n}_a(z) \bar{n}_b(z) R_{ab}, \quad R_{ab} = \int dx [\phi_a^2(x) \phi_b'(x)^2 - \phi_a(x) \phi_a'(x) \phi_b(x) \phi_b'(x)]. \quad (\text{B31})$$

Note that  $J_{ab} = R_{ab} + R_{ba}$ .

At fixed complex fugacity  $z$ , the occupation numbers are independent (the kernel form is exact), so the integrand is well-defined. The contour integral projects onto the  $N$ -particle sector.

### Appendix C: Numerical procedure

Our goal here is to provide details on the numerical procedures to compute the contact from eq. (5). We begin by defining the matrix

$$R_{ab} = \int_{-\infty}^{\infty} dx [\phi_a(x)^2 \phi_b'(x)^2 - \phi_a(x) \phi_a'(x) \phi_b(x) \phi_b'(x)], \quad (\text{C1})$$

truncated to  $M$  single-particle levels ( $a, b = 0, \dots, M-1$ ) and evaluated by the trapezoidal rule on a uniform grid of  $N_x = \max(4000, 6M)$  points spanning  $[-L, L]$  with  $L = \sqrt{2M} + 6$ . The wave functions  $\phi_n(x)$  and their derivatives are generated via the three-term recurrence

$$\phi_{n+1}(x) = \sqrt{\frac{2}{n+1}} x \phi_n(x) - \sqrt{\frac{n}{n+1}} \phi_{n-1}(x), \quad \phi_n'(x) = \sqrt{\frac{n}{2}} \phi_{n-1}(x) - \sqrt{\frac{n+1}{2}} \phi_{n+1}(x). \quad (\text{C2})$$

With the arrays  $\phi_a(x_i)$  and  $\phi_a'(x_i)$  precomputed,  $R_{ab}$  is assembled as  $R = P - Q$  via dense matrix products of cost  $\mathcal{O}(M^2 N_x)$ .

The canonical contact is expressed as a ratio of contour integrals,

$$\mathcal{C}_N = \frac{2}{\pi} \text{Re} \left[ \frac{\frac{1}{N_\theta} \sum_{k=0}^{N_\theta-1} W_k G_k e^{-iN\theta_k}}{\frac{1}{N_\theta} \sum_{k=0}^{N_\theta-1} W_k e^{-iN\theta_k}} \right], \quad (\text{C3})$$

with  $\theta_k = 2\pi k / N_\theta$ , contour points  $z_k = r e^{i\theta_k}$ , and

$$W_k = \exp[\log \Xi(z_k) - \log \Xi(z_0)], \quad G_k = \sum_{a,b=0}^{M_{\text{use}}-1} \bar{n}_a(z_k) \bar{n}_b(z_k) R_{ab}. \quad (\text{C4})$$

Here  $\Xi(z) = \prod_{n=0}^{M-1} (1 + z e^{-\beta \varepsilon_n})$ ,  $\bar{n}_a(z) = z e^{-\beta \varepsilon_a} / (1 + z e^{-\beta \varepsilon_a})$ , and the saddle-point radius  $r = e^{\beta \mu}$  is determined by  $\sum_n \bar{n}_n(r) = N$ . The number of contour points  $N_\theta$  is chosen large enough that doubling it changes  $\mathcal{C}_N$  in (C3) by less than  $10^{-5}$  in relative units; in practice  $N_\theta = 256$  is sufficient for  $N \leq 100$  across the entire  $\tau \in [0, 10]$  window.

Crucially, the partition function  $\Xi(z)$  and the saddle-point condition use all  $M_{\text{full}} = N + 14 \tau N + 20$  levels needed for convergence (the coefficient 14 corresponds to retaining levels with Boltzmann weight as low as  $e^{-14} \sim 10^{-6}$  at the highest relevant temperature; the additive offset 20 handles the low- $\tau$  band edge), while the spatial integral  $G_k$  uses only  $M_{\text{use}} = \min(M_{\text{full}}, M_{\text{max}})$  levels, where  $M_{\text{max}}$  is the size of the precomputed  $R$  matrix. This ensures the entire calculation remains in the canonical ensemble—no grand-canonical fallback is used.

### a. Spatial truncation at high $\tau$

The spatial truncation in  $G_k$  deserves careful comment, because its behaviour at high  $\tau$  is more subtle than a naive per-level estimate suggests. A first-pass bound on the truncation error is the occupation of the highest retained level at the saddle,  $\bar{n}_{M_{\text{max}}}(r)$ . At the worst corner ( $N = 100$ ,  $\tau = 10$ ) with  $M_{\text{max}} = 4000$  this gives  $\bar{n}_{M_{\text{max}}} \sim 10^{-3}$ , suggesting a relative deviation of order  $10^{-3}$ . The actual truncation error at that corner is closer to 15%. The discrepancy arises because the spatial matrix elements  $R_{ab}$  in (C1) grow as  $\sqrt{ab}$  for large indices, so the contribution of pairs  $(a, b)$  with  $a, b \gtrsim M_{\text{max}}$  is enhanced by a factor  $\sqrt{ab}$  relative to the bare occupation, and the number of contributing pairs is  $\sim (M_{\text{full}} - M_{\text{max}})^2$ . The cumulative truncation therefore scales linearly in  $1 - M_{\text{max}}/M_{\text{full}}$  rather than with the per-level occupation.

The empirically clean criterion for  $G_k$  to reproduce the full-level result to better than  $\sim 0.05\%$  is

$$M_{\text{max}} \geq 1.2 M_{\text{full}}(N, \tau) = 1.2 (N + 14 \tau N + 20). \quad (\text{C5})$$

Below this threshold the truncation bias is monotonic and well-modelled by  $\mathcal{C}_N^{(M_{\text{max}})} / \mathcal{C}_N^{(\infty)} \simeq 1 - c_\tau (1 - M_{\text{max}}/M_{\text{full}})$  with  $c_\tau \sim \mathcal{O}(1)$  and weakly  $\tau$ -dependent. Crossing  $M_{\text{max}} = M_{\text{full}}$  produces the step transition to the converged value: at ( $N = 20$ ,  $\tau = 10$ ,  $M_{\text{full}} = 2840$ ), raising  $M_{\text{max}}$  from 2000 ( $M_{\text{max}}/M_{\text{full}} = 0.70$ ) to 2840 shifts  $\mathcal{C}_N^{(M_{\text{max}})}$  from 978.87 to 979.10, where it plateaus (979.10 at  $M_{\text{max}} = 3500$ ). This is the converged value; the prediction of the scaling law (12), 979.27, then differs from it by 0.02%, consistent with the expected  $\mathcal{O}(N^{-1})$  subleading corrections to the scaling law.

This  $\tau$ -dependent saturation is the reason the high- $\tau$  ratio plot behaves differently from the low- $\tau$  one even at fixed  $M_{\text{max}}$ . At  $\tau = 0.05$  and  $N = 100$ ,  $M_{\text{full}} = 190$ , so any  $M_{\text{max}} \gtrsim 250$  saturates the criterion (C5) and the plot collapses cleanly to unity. At  $\tau = 10$  and the same  $N$ ,  $M_{\text{full}} = 14,120$ , so  $M_{\text{max}} = 4000$ – $5000$  is well below threshold and the truncation bias dominates the apparent residual. We therefore restrict the high- $\tau$  verification plot to the  $(N, \tau)$  corner satisfying (C5) for the chosen  $M_{\text{max}}$ ; in this corner the ratio  $\mathcal{R}_N$  defined in (68) collapses to unity to within 0.05–0.2% for all  $N \geq 5$  and  $\tau \in [5, 10]$ , which is consistent with the genuine  $\mathcal{O}(N^{-1})$  finite-size corrections (recall: the  $N^{1/2}$  term contributes  $\sim 1\%$  at  $N = 20$ , dropping to  $\sim 0.05\%$  at  $N = 100$ ). Extending the plot to higher  $N$  at fixed high  $\tau$  requires bumping  $M_{\text{max}}$  in proportion to  $\tau N$ .

## 1. Scaling verification

We verify the scaling ansatz (12) by comparing the numerical data against the asymptotic predictions in the low- and high- $\tau$  regimes, and against the exact numerical evaluation of the integral representations at intermediate  $\tau$ . All figures in the main text were generated with  $M_{\text{max}} = 5000$  single-particle levels. This satisfies the safety criterion (C5) on the union of windows displayed in Figs. 1, 2, 3, 4a, and 4b; the corner ( $N = 100$ ,  $\tau = 10$ ) requires  $M_{\text{max}} \approx 17,000$  for the same relative truncation accuracy and is therefore excluded from Fig. 3 (see the discussion below eq. (C5)).

The scaling functions  $A(\tau)$  and  $B(\tau)$  are computed from (32) and (67), respectively, with the Fermi factor (25) evaluated at the self-consistent scaled chemical potential  $\xi(\tau)$  determined by (26).

The closed asymptotic forms used to anchor the verification are: for  $A(\tau)$ , the Sommerfeld expansion (39) at low  $\tau$  and the virial expansion (51) at high  $\tau$ ; for  $B(\tau)$ , the Sommerfeld result (91) at low  $\tau$  and the virial result (103) at high  $\tau$ . At intermediate  $\tau \sim 1$ , the integrals (32) and (67) are evaluated numerically using adaptive Gauss–Kronrod quadrature for the inner  $q$ -integrals and Gauss–Legendre quadrature for the outer  $u$ -integral.

## 2. Padé approximants

### a. Leading coefficient

We write

$$A_{\text{P}}(\tau) = \frac{a_0 (1 + \tilde{\alpha} \tau^2)}{(1 + \beta \tau^2)^{3/4}} \times \left[ 1 + \frac{c \tau^2}{(1 + d \tau)^3} + \frac{e \tau^3}{(1 + d \tau)^4} \right], \quad (\text{C6})$$

where  $a_0 = 128\sqrt{2}/(45\pi^3)$ . The base factor (first fraction) is a generalised Padé with fractional exponent 3/4 in the denominator, which produces the correct  $\sqrt{\tau}$  growth at large  $\tau$ . The multiplicative correction (square bracket) acts as a localised ‘‘bump’’ that equals unity at both  $\tau = 0$  and  $\tau \rightarrow \infty$ , and improves accuracy in the crossover region  $\tau \sim 1$ .

The parameter  $\beta$  is determined analytically. At small  $\tau$ , expanding (C6) gives  $A_{\text{P}} = a_0[1 + (\tilde{\alpha} - \frac{3}{4}\beta + c)\tau^2 + \mathcal{O}(\tau^3)]$ , so setting  $\tilde{\alpha} = a_2/a_0 + \frac{3}{4}\beta - c$  enforces the Sommerfeld result (39). At large  $\tau$ ,  $A_{\text{P}} \rightarrow a_0 \tilde{\alpha}/\beta^{3/4} \sqrt{\tau}$ , so matching (51) requires  $a_0 \tilde{\alpha}/\beta^{3/4} = 1/\pi^{3/2}$ . Eliminating  $\tilde{\alpha}$  yields a quartic for  $t := \beta^{1/4}$ :

$$\frac{3a_0}{4} t^4 - \frac{t^3}{a_0 \pi^{3/2}} + \frac{a_2}{a_0} = 0, \quad \beta = t^4, \quad (\text{C7})$$

whose smallest positive root gives  $\beta \approx 0.0798$ . The remaining parameters are obtained by minimax fit (minimising the maximum relative error) to the numerical evaluation of (32):

$$c = 1.4435, \quad e = 2.000, \quad d = 0.8793. \quad (\text{C8})$$

The resulting maximum relative error of  $A_{\text{P}}(\tau)$  with respect to the numerical evaluation of (32) is

$$\max_{\tau \in [0, 10]} \left| \frac{A_{\text{P}}(\tau) - A(\tau)}{A(\tau)} \right| \simeq 4.5\%, \quad (\text{C9})$$

with the worst-case location in the crossover region  $\tau \sim 1$ .

### b. Subleading coefficient

For  $B(\tau)$  we use a form that respects both the linear low- $\tau$  slope and the  $\sqrt{\tau}$  high- $\tau$  asymptote. Setting  $\sigma := \sqrt{\tau}$ , we write

$$B_{\text{P}}(\tau) = -\frac{\sigma}{\pi^{3/2}} \frac{a_1 \sigma + a_2 \sigma^2 + a_3 \sigma^3 + a_4 \sigma^4}{1 + d_1 \sigma + d_2 \sigma^2 + d_3 \sigma^3 + d_4 \sigma^4}, \quad (\text{C10})$$

with two analytic constraints fixing the asymptotic behaviour:

$$a_1 = -\pi^{3/2} b_1 = \frac{16\sqrt{2}}{3\pi^{3/2}} \simeq 1.3545, \quad a_4 = d_4, \quad (\text{C11})$$

where the first constraint enforces the Sommerfeld leading slope  $B(\tau) \rightarrow b_1 \tau$  from (91) and the second enforces  $B_{\text{P}}(\tau) \rightarrow -\sqrt{\tau}/\pi^{3/2}$  at large  $\tau$  from (103). The remaining parameters  $a_2, a_3, d_1, d_2, d_3, d_4$  are determined by minimax fit to the numerical evaluation of (67) on  $\tau \in [0.01, 10]$ :

$$\begin{aligned} a_2 &= -0.4116, & a_3 &= 0.5126, & a_4 &= 8.6085, \\ d_1 &= -0.3860, & d_2 &= 1.7283, & d_3 &= 0.2215, & d_4 &= 8.6085. \end{aligned} \quad (\text{C12})$$

The resulting maximum relative error of  $B_{\text{P}}(\tau)$  with respect to the numerical evaluation of (67) is

$$\max_{\tau \in [0.01, 10]} \left| \frac{B_{\text{P}}(\tau) - B(\tau)}{B(\tau)} \right| \simeq 0.13\%, \quad (\text{C13})$$

with the worst-case location at the boundaries of the fitting interval. The form (C10) is asymptotically correct in both regimes by construction: numerically,  $B_{\text{P}}(\tau) \rightarrow -\sqrt{\tau}/\pi^{3/2}$  to within 0.1% already by  $\tau = 10$ , and the extrapolation

remains accurate indefinitely (at  $\tau = 100$ ,  $B_P \simeq -1.798$  versus  $-\sqrt{100}/\pi^{3/2} \simeq -1.796$ ). The Padé (C10) is therefore a uniformly valid closed-form substitute for the integral representation (67) across the full physical temperature window.

In analogy with the ratio  $\mathcal{R}_N$  defined in (68), we introduce its Padé counterpart

$$\mathcal{R}_N^{(P)}(\tau) := \frac{\mathcal{C}_N(\tau)}{A_P(\tau) N^{5/2} + B_P(\tau) N^{3/2}}, \quad (\text{C14})$$

in which the universal scaling functions  $A(\tau)$  and  $B(\tau)$  are replaced by their Padé approximants  $A_P(\tau)$  and  $B_P(\tau)$  from (C6) and (C10).

- 
- [1] S. Tan, *Ann. Phys. (N.Y.)* **323**, 2952 (2008).
  - [2] S. Tan, *Ann. Phys. (N.Y.)* **323**, 2971 (2008).
  - [3] S. Tan, *Ann. Phys. (N.Y.)* **323**, 2987 (2008).
  - [4] E. Braaten and L. Platter, *Phys. Rev. Lett.* **100**, 205301 (2008).
  - [5] E. Braaten, D. Kang, and L. Platter, *Phys. Rev. Lett.* **106**, 153005 (2011).
  - [6] S. Zhang and A. J. Leggett, *Phys. Rev. A* **79**, 023601 (2009).
  - [7] F. Werner and Y. Castin, *Phys. Rev. A* **86**, 013626 (2012).
  - [8] F. Werner and Y. Castin, *Phys. Rev. A* **86**, 053633 (2012).
  - [9] R. Combescot, F. Alzetto, and X. Leyronas, *Phys. Rev. A* **79**, 053640 (2009).
  - [10] J. T. Stewart, J. P. Gaebler, T. E. Drake, and D. S. Jin, *Phys. Rev. Lett.* **104**, 235301 (2010).
  - [11] E. D. Kuhnle, H. Hu, X.-J. Liu, P. Dyke, M. Mark, P. D. Drummond, P. Hannaford, and C. J. Vale, *Phys. Rev. Lett.* **105**, 070402 (2010).
  - [12] Y. Sagi, T. E. Drake, R. Paudel, and D. S. Jin, *Phys. Rev. Lett.* **109**, 220402 (2012).
  - [13] R. J. Wild, P. Makotyn, J. M. Pino, E. A. Cornell, and D. S. Jin, *Phys. Rev. Lett.* **108**, 145305 (2012).
  - [14] E. H. Lieb and W. Liniger, *Phys. Rev.* **130**, 1605 (1963).
  - [15] E. H. Lieb, *Phys. Rev.* **130**, 1616 (1963).
  - [16] C. N. Yang and C. P. Yang, *J. Math. Phys.* **10**, 1115 (1969).
  - [17] M. D. Girardeau, *J. Math. Phys.* **1**, 516 (1960).
  - [18] M. Olshanii, *Phys. Rev. Lett.* **81**, 938 (1998).
  - [19] M. A. Cazalilla, R. Citro, T. Giamarchi, E. Orignac, and M. Rigol, *Rev. Mod. Phys.* **83**, 1405 (2011).
  - [20] B. Paredes, A. Widera, V. Murg, O. Mandel, S. Fölling, I. Cirac, G. V. Shlyapnikov, T. W. Hänsch, and I. Bloch, *Nature (London)* **429**, 277 (2004).
  - [21] T. Kinoshita, T. Wenger, and D. S. Weiss, *Science* **305**, 1125 (2004).
  - [22] T. Kinoshita, T. Wenger, and D. S. Weiss, *Phys. Rev. Lett.* **95**, 190406 (2005).
  - [23] E. Haller, M. Gustavsson, M. J. Mark, J. G. Danzl, R. Hart, G. Pupillo, and H.-C. Nägerl, *Science* **325**, 1224 (2009).
  - [24] T. Jacqmin, J. Armijo, T. Berrada, K. V. Kheruntsyan, and I. Bouchoule, *Phys. Rev. Lett.* **106**, 230405 (2011).
  - [25] A. Vogler, R. Labouvie, F. Stubenrauch, G. Barontini, V. Guarrera, and H. Ott, *Phys. Rev. A* **88**, 031603(R) (2013).
  - [26] J. M. Wilson, N. Malvania, Y. Le, Y. Zhang, M. Rigol, and D. S. Weiss, *Science* **367**, 1461 (2020).
  - [27] N. Malvania, Y. Zhang, Y. Le, J. Dubail, M. Rigol, and D. S. Weiss, *Science* **373**, 1129 (2021).
  - [28] Q. Huang, H. Yao, X. Chen, and L. Sanchez-Palencia, *Sci. Adv.* **11**, eadv3727 (2025).
  - [29] A. Minguzzi, P. Vignolo, and M. P. Tosi, *Phys. Lett. A* **294**, 222 (2002).
  - [30] M. Olshanii and V. Dunjko, *Phys. Rev. Lett.* **91**, 090401 (2003).
  - [31] M. Barth and W. Zwerger, *Ann. Phys. (N.Y.)* **326**, 2544 (2011).
  - [32] K. V. Kheruntsyan, D. M. Gangardt, P. D. Drummond, and G. V. Shlyapnikov, *Phys. Rev. Lett.* **91**, 040403 (2003).
  - [33] P. Vignolo and A. Minguzzi, *Phys. Rev. Lett.* **110**, 020403 (2013).
  - [34] H. Yao, D. Clément, A. Minguzzi, P. Vignolo, and L. Sanchez-Palencia, *Phys. Rev. Lett.* **121**, 220402 (2018).
  - [35] G. Lang, P. Vignolo, and A. Minguzzi, *Eur. Phys. J. Spec. Top.* **226**, 1583 (2017).
  - [36] J. Decamp, J. Jünemann, M. Albert, M. Rizzi, A. Minguzzi, and P. Vignolo, *Phys. Rev. A* **94**, 053614 (2016).
  - [37] J. Decamp, M. Albert, and P. Vignolo, *Phys. Rev. A* **97**, 033611 (2018).
  - [38] M. Rizzi, C. Miniatura, A. Minguzzi, and P. Vignolo, *Phys. Rev. A* **98**, 043607 (2018).
  - [39] F. T. Sant'Ana, F. Hébert, V. G. Rousseau, M. Albert, and P. Vignolo, *Phys. Rev. A* **100**, 063608 (2019).
  - [40] A. Minguzzi and P. Vignolo, *AVS Quantum Sci.* **4**, 027102 (2022).
  - [41] L. D. Cloutman, *Astrophys. J. Suppl. Ser.* **71**, 677 (1989).
  - [42] R. B. Dingle, *Asymptotic Expansions: Their Derivation and Interpretation* (Academic Press, London, 1973).
  - [43] R. Kubo, H. Ichimura, T. Usui, and N. Hashitsume, *Statistical Mechanics: An Advanced Course with Problems and Solutions* (North-Holland, Amsterdam, 1965).
  - [44] H. Touchette, *Phys. Rep.* **478**, 1 (2009).